


ORIGINAL ARTICLE

Open Access

# Superlubricity of molybdenum disulfide film



Hongxuan Li<sup>1,2\*</sup> , Shifan Ju<sup>1,2</sup>, Li Ji<sup>1,2</sup>, Xiaohong Liu<sup>1,2</sup>, Huidi Zhou<sup>1,2</sup>, Jianmin Chen<sup>1,2</sup> and Xiaoqin Zhao<sup>1,2\*</sup>

## Abstract

Superlubricity is an ideal state with zero contact friction between two frictional interfaces. It has become a hot research topic for many scientists in the past 20 years, and the field spans the complex hot research directions of physics, chemistry, mechanics, and materials. The concept of superlubricity was introduced in 1990, and the understanding of the process of realizing superlubricity is vital for controlling the tribological properties of materials and promoting the development of tribology. This review focuses on the fundamental properties of molybdenum disulfide (MoS<sub>2</sub>) films and the influence of the environment on affecting MoS<sub>2</sub> films. As a result, some methods for realizing superlubricity by MoS<sub>2</sub> films are proposed. The key to achieving superlubricity with MoS<sub>2</sub> is summarized. Finally, an outlook on the application of MoS<sub>2</sub> films is given.

**Keywords** MoS<sub>2</sub>-based films, Superlubricity, Tribological properties, Incommensurate contact

## 1 Introduction of Superlubricity

Friction and wear are caused by the bite of contact areas between two uneven solid surfaces during contact sliding. The greater the pressure between the two planes, the greater the contact area and the more severe the bite, resulting in greater friction and wear. When the friction between two smooth contact planes is zero, an ideal state is created, called superlubricity. However, this ideal state does not exist in reality, so when the coefficient of friction is lower than 0.01, it is considered that the superlubricative state is reached [1, 2]. The study of superlubricity is beneficial to reduce friction-induced wear, which significantly impacts energy saving, environmental protection, technological innovation, and economic development. The study of superlubricity is also very challenging in the subject of tribology. Therefore, many researchers have

tried to go farther in this direction and realize superlubricity by various methods. Solid lubricant materials that can achieve superlubricity so far are mainly classified into two kinds: 1) ordered two-dimensional (2D) materials, such as MoS<sub>2</sub>, graphite, graphene, etc. [3–8] 2) amorphous materials, such as diamond-like carbon (DLC) and amorphous MoS<sub>2</sub> [9–11]. Due to the different application environments of MoS<sub>2</sub> and DLC films, space solid lubrication materials are mainly based on MoS<sub>2</sub>-based films because of the poor performance of DLC films in a vacuum. MoS<sub>2</sub> has a particular layer structure, which makes MoS<sub>2</sub> extremely susceptible to relative slippage between layers under the action of low shear in the friction process [12]. This fundamental property gives MoS<sub>2</sub> excellent frictional properties in ultra-high vacuum and inert gas environments. The study of the superlubricative behavior and mechanism of MoS<sub>2</sub> is conducive to better developing new space solid lubrication materials.

The tribological properties of films are usually studied in terms of the chemical-physical changes at the friction interface and the structure and composition of the film. The study of film superlubricity is no exception. The physicochemical state of the film plays a decisive role in its tribological properties. Since the MoS<sub>2</sub> layers are connected by weak van der Waals forces and the atoms within the layers are connected by strong covalent bonds, it is easy for this material to slide between

\*Correspondence:

Hongxuan Li  
lihx@licp.cas.cn  
Xiaoqin Zhao

zhaoxiaoqin@licp.cas.cn

<sup>1</sup> State Key Laboratory of Solid Lubrication, Lanzhou Institute of Chemical Physics, Chinese Academy of Sciences, No.18, Tianshui Middle Road, Lanzhou 730000, China

<sup>2</sup> Center of Materials Science and Optoelectronics Engineering, University of Chinese Academy of Sciences, No.1, Yanqi Lake East Road, Beijing 100049, Huairou District, China

the layers when subjected to shear force and obtain a low coefficient of friction. Therefore, controlling the structure of the MoS<sub>2</sub>-based friction interface becomes essential to realizing the superlubricity of MoS<sub>2</sub>-based films. In addition, the interaction between the frictional interface of the film and the environment is also crucial to the frictional properties of the film, and the tribological properties of MoS<sub>2</sub> films are susceptible to environmental conditions. In general, in a high vacuum and dry inert atmosphere, MoS<sub>2</sub> films exhibit ultra-low friction and wear. The friction coefficient is elevated in the presence of O<sub>2</sub>, water, etc. [13], and wear increases. Therefore, constructing a weak chemical interaction at the friction interface is also a means to achieve superlubricity.

In order to realize superlubricity, it is first necessary to realize the modulation of the friction interface and the establishment of a weak chemical environment. Firstly, we introduced the structure and preparation of MoS<sub>2</sub> films. In the second section, the three means to realize the superlubricity of MoS<sub>2</sub> are introduced (as summarized in Fig. 1), followed by the influence of the environment on the realization of the superlubricity of MoS<sub>2</sub> in the third section. Finally, an outlook on the development of MoS<sub>2</sub> lubricated films is given.

### 2 Structure and tribological applications of MoS<sub>2</sub>

The molecular structure of MoS<sub>2</sub> is shown in Fig. 2 (a), and the thickness of each two-dimensional crystal layer is about 0.65nm. Van der Waals forces bind together these

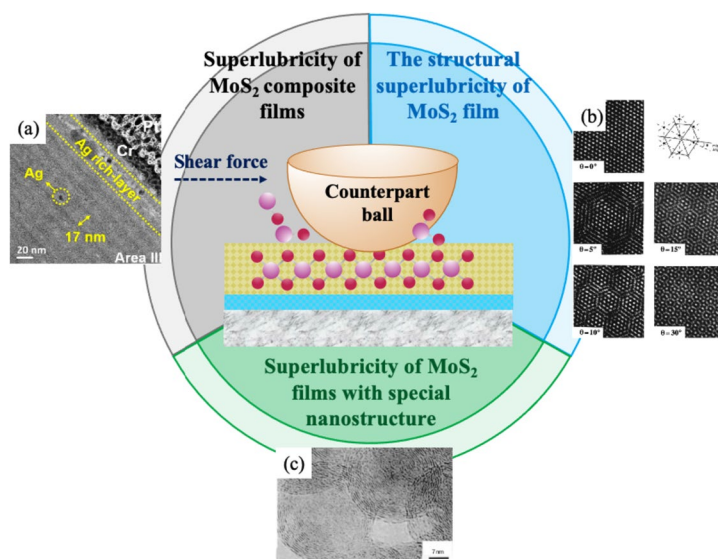


**Fig. 1** Schematic representation of the main routes to superlubricity in MoS<sub>2</sub> films; HRTEM analysis of the wear track of MoS<sub>2</sub>-Ag films (a) [14]. Computational simulations showing the interference between two single-hexagonal lattices superposed at different rotation angles (b) [15]. HRTEM images of fullerene-like MoS<sub>2</sub> nanofilms (c) [16]. (a) reproduced from ref. 33. Copyright © 2021 American Chemical Society; (b) reproduced from ref. 12. Copyright © 2007 Elsevier B.V.; (c) reproduced from ref. 20. Copyright © 2000 Macmillan Magazines Ltd

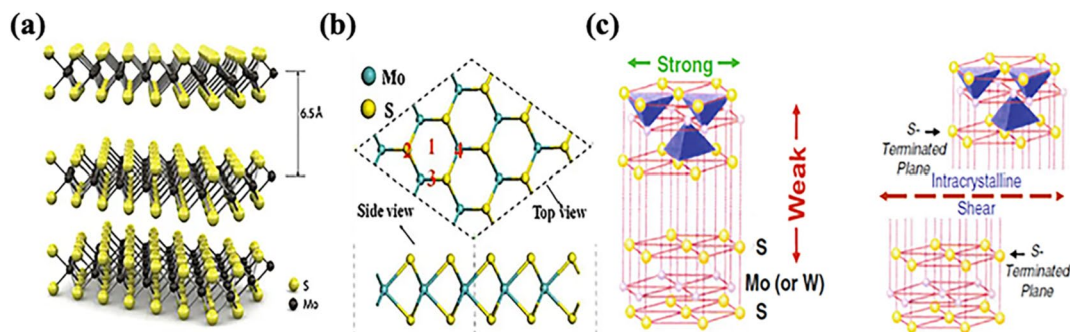


**Fig. 2** Schematic structure of MoS<sub>2</sub> material [17, 18]. a and b reproduced from ref. 1. Copyright ©2011 Nature Publishing Group; c reproduced from ref. 3. Copyright ©2012 J Mater Sci

layers, so a single layer of MoS<sub>2</sub> alkene can be obtained by micromechanical exfoliation. Each two-dimensional crystal layer of MoS<sub>2</sub> has a plane of Mo atoms arranged in a hexagonal shape sandwiched between two planes of S atoms arranged in a hexagonal shape, as shown in Fig. 2 (b), and covalently bonded. The S-Mo-S atoms are arranged in a trigonal shape to form a hexagonal crystal structure. The MoS<sub>2</sub> structure is an octahedral crystal symmetry structure with a Mo-S bond length of 2.4Å, a lattice constant of 3.2Å, and an upper and lower S-atom spacing of 3.1Å [17].

MoS<sub>2</sub> powder is blackish gray, slightly blue, with a slippery feeling. Natural MoS<sub>2</sub> is the main component of molybdenite, with a density of 4.5~4.8g/cm<sup>3</sup>, a melting point of 1185°C, a Mohs hardness of 1.0~1.5, a coefficient of thermal expansion of 10.7×10<sup>-6</sup>/K, and a certain degree of magnetism. Its chemical properties are stable, except for aqua regia, concentrated hot hydrochloric acid, nitric acid, and sulfuric acid; it cannot be dissolved in other acids and bases, pharmaceuticals, solvents, water, petroleum products, and synthetic lubricants. MoS<sub>2</sub> begins to oxidize at 350°C in air, and intense oxidation occurs after 516°C, and it maintains a stable structure at 900°C in an ultra-high vacuum and inert gas [19].

Since the MoS<sub>2</sub> layers are connected by weak van der Waals forces and the atoms in the layers are connected by strong covalent bonds, this material is easy to slide between the layers when subjected to shear and obtains a low coefficient of friction (Fig. 2 (c)) [18]. Therefore, MoS<sub>2</sub> is widely used as an excellent solid lubricant material known as the "king of solid lubrication".

This section focuses on the superlubricative behavior and tribological properties of sputtered MoS<sub>2</sub> films. MoS<sub>2</sub> films were first prepared on Nb and Ni–Cr surfaces by T. Spalvins [20] in 1969 using DC sputtering with uniform composition and thickness, good bonding to the substrate, demonstrating low friction and long life under vacuum, and good reproducibility of film preparation and experiments. Since then, the sputtered MoS<sub>2</sub> film technology has rapidly developed and has become the preferred method for preparing films of TMDs (Transition Metal Dichalcogenides). It is widely used in aerospace and other industrial applications.

MoS<sub>2</sub> films can be categorized into four types based on their crystal orientation on the substrate surface [21]. The first type is MoS<sub>2</sub> crystals with (002) basal plane parallel to the substrate surface (basal orientation). The second type is MoS<sub>2</sub> crystals with the (002) basal plane perpendicular to the substrate surface, where the (100) and (110) planes of MoS<sub>2</sub> microcrystals are parallel to the substrate surface (edge orientation). The third category can be regarded as a mixture of the first and second categories and is also known as randomly oriented films, i.e.,

the coexistence of basal plane-oriented microcrystals and edge-oriented microcrystals (random orientation) in the films. The fourth type of film is amorphous structures.

In general, most sputter-deposited MoS<sub>2</sub> films show edge-oriented structures [22]. Bertrand proposed the theory of active-site nucleation [23]: During film deposition, the active sites on the substrate react with the S atoms in the plasma, and a large number of reactive S atoms exist on the edge planes, which are prone to bond with other atoms on the deposition surface. The directionality of the S suspension bonds forces the formation of edge-oriented films. Hilton showed by TEM analysis that MoS<sub>2</sub> consists of edge and basal plane-oriented islands in the early stage of film growth. Since the growth rate of edge orientation is faster than that of the basal plane, the edge-oriented islands dominate the film, which in turn obscures and inhibits the continued growth of the basal plane-oriented islands, and the film ultimately forms an edge-oriented structure [24].

Since no vacant orbitals or dangling bonds exist on the basal plane, forming strong chemical bonds between the microcrystalline basal plane and the substrate is impossible. As a result, films with a basal plane parallel to the surface of the substrate (basal plane orientation) will not adhere well to the substrate. However, films with a basal plane orientation have better cohesion and densification and, therefore, better resistance to oxygen and moisture. In contrast, films with edge orientation are oxidized easily and are very sensitive to humidity. Scharf pointed out [18] that regardless of the type of pristine sputtered MoS<sub>2</sub> film, during friction, the frictional stresses can reorient the MoS<sub>2</sub> crystals to form ordered (002) crystalline surfaces at the friction interface parallel to the sliding direction.

The most important application area for MoS<sub>2</sub> films is space technology, which involves a variety of harsh environments such as ultra-high vacuum, high and low-temperature alternations, atomic oxygen (AO), and intense irradiation. Liquid lubricants evaporate and may contaminate equipment in high vacuum, decompose or oxidize at high temperatures, solidify and fail to lubricate at low temperatures, disintegrate under intense irradiation, and are extruded from contact surfaces under high loads, making it challenging to meet the lubrication needs of space equipment. In particular, liquid lubricants require complex oiling and sealing devices for space equipment, resulting in higher weight and degradation with prolonged use or storage and inactivity. MoS<sub>2</sub> films overcome the above problems and are widely used in bearings, gears, pointing mechanisms, slip rings, and release mechanisms of space vehicles. Almost all satellites and spacecraft use MoS<sub>2</sub> film lubrication treatments [25].

The latest typical space application for MoS<sub>2</sub> films, the James Webb Space Telescope (JWST), is given here. It is one of the most complex projects in NASA's history, and because it is too far from Earth to send astronauts for maintenance, it must be designed and built flawlessly, or it will be a lost cause! MoS<sub>2</sub> films have been identified as the preferred solid lubricant for the focusing and aligning mechanisms of many precision instruments on the JWST, including the focusing and alignment mechanisms of the Near Infrared Camera (NIRCam), and the Mid-Infrared Instrument (MIRI), the gear on the Fine Guidance Sensor (FGS) as the solid lubricant of choice [25, 26]. The key to selecting MoS<sub>2</sub> film as the solid lubricant of choice for these high-precision instruments is its ability to maintain its lubricating properties at low temperatures (30K, the operating temperature of the JWST) and its ability to be deposited on precision bearings at sub-micrometer thicknesses to ensure their stable operation (as shown in Fig. 3). To be sure, the MoS<sub>2</sub> film-lubricated bearings were subjected to extensive tests on the ground to evaluate their tribological properties under various operating conditions to ensure reliability for end-use in space. For example, the MoS<sub>2</sub> film plated on the focusing and alignment mechanism of the infrared camera had to undergo a life test of 200,000 revolutions in an ultra-low-temperature environment, with a repeatable positional accuracy of less than 4 $\mu$ m, and an increase in threshold motor current of less than 30%. Various MoS<sub>2</sub> films underwent atmospheric storage tests for more than four years to verify the effect of ground storage on their lifetime [27, 28].

The James Webb Space Telescope was launched at 20:20 on 25 December 2021 aboard an Ariane 5 launch vehicle from the Kourou Space Launch Centre in Guiana, and the telescope was officially operational in July 2022, when it photographed the famous "Pillars of Creation," illustrating yet another successful application of lubricated MoS<sub>2</sub> films in space.

### 3 Superlubricative mechanism of MoS<sub>2</sub> films

#### 3.1 The structural superlubricity of MoS<sub>2</sub> films

The superlubricative behavior of MoS<sub>2</sub> films was first discovered by the team of C. Donnet and J. M. Martin in 1992 [30]. They built an ultra-high vacuum (UHV) in-situ film preparation, structural analysis, and friction test rig, as shown in Fig. 4 (a). The substrate enters the film preparation chamber through a transition chamber (9), is cleaned with ion etching (10), and then a MoS<sub>2</sub> film is deposited using a PVD source (14). After film deposition, it was transferred to the main UHV chamber to start the pin-disk friction test (1, 2, 3). Before and after friction, the original structure of the films and the abrasion marks can be structurally analyzed using XPS (17, 19) and AES (16, 17). The equipment enables in-situ preparation, friction testing, and structural analysis of MoS<sub>2</sub> films under ultra-high vacuum conditions, thus avoiding adsorption effects such as atmospheric water vapor and oxygen. Donnet deposited a 120nm thick film of pure MoS<sub>2</sub> on the surface of Si, which has an S: Mo ratio of 2.04, basically by the stoichiometric ratio of MoS<sub>2</sub>. The TEM analysis shows that there are (002) basal, (100), and (110) prismatic surfaces in the films, which are edge-oriented structures. The friction behavior of the films in ultrahigh vacuum was investigated using a pin-disk friction tester, with a pin using an  $\alpha$ -SiC hemisphere with a radius of curvature of 2mm, a load of 1N (contact pressure of 0.66GPa), a linear velocity of 0.5mm/s, a reciprocating length of 3mm, and a vacuum degree of  $5 \times 10^{-10}$ Torr. The results show that the films have a superlubricative friction coefficient of 0.003, which is one order of magnitude lower than that of the previously reported friction coefficient one order of magnitude lower than that reported. The authors concluded that forming a (002) base surface parallel to the sliding direction during friction, frictional anisotropy, and the absence of contamination, such as water vapor and oxygen, are the critical factors for superlubricity.

Subsequently, J. M. Martin prepared 120nm thick MoS<sub>2</sub> films on AISI 52100 steel using the same

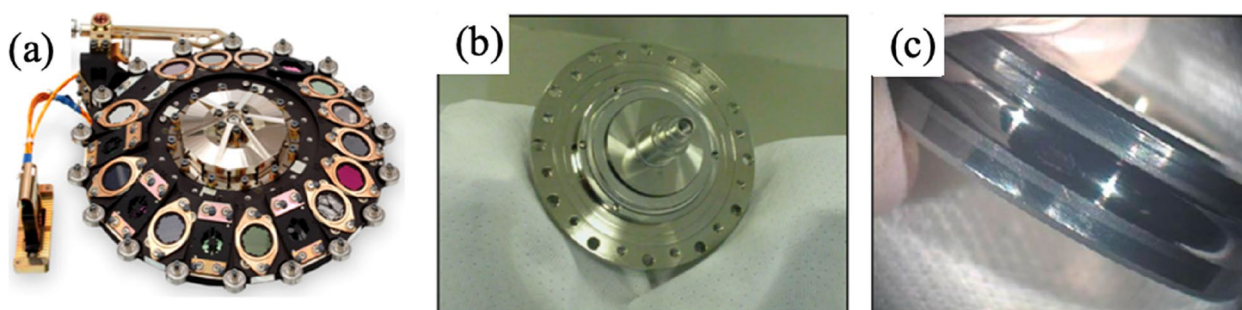


**Fig. 3** Application of MoS<sub>2</sub> films on JWST bearing (a) MIRI instrument filter wheel assembly (b) Filter wheel assembly bearing (c) lubricated bearing with MoS<sub>2</sub> films [26, 29]. a and b reproduced from ref. 122. Copyright ©2010 SPIE; (c) reproduced from ref. 119. Copyright ©2012 IOP



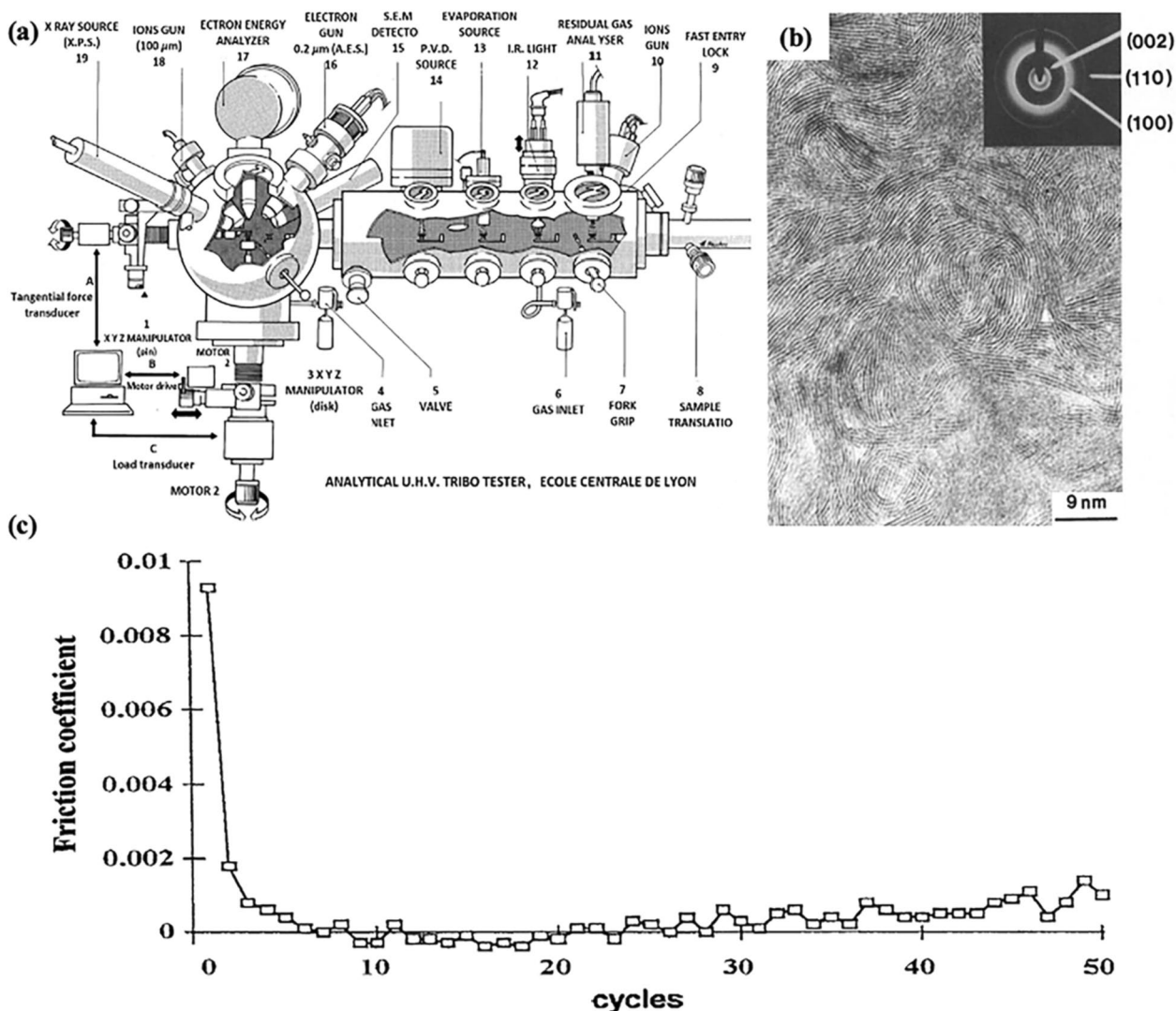


**Fig.4** Schematic diagram of ultra-high vacuum in-situ film preparation, structural analysis, and friction test equipment (a) [30], HRTEM photo of MoS<sub>2</sub> film (b) [31], friction coefficient variation curve of MoS<sub>2</sub> film (c) [1, 15] (a) reproduced from ref. 11. Copyright ©1994 Surface and Coatings Technology; (b) reproduced from ref. 11. Copyright ©2022 Surface and Coatings Technology; (c) reproduced from ref. 12. Copyright © 2007 Elsevier B.V. All rights reserved

equipment [1, 15, 31] and examined the frictional behavior in ultrahigh vacuum in situ using a pin-disc reciprocating friction tester. The test conditions were a steel hemisphere with a 4mm radius of curvature for the pin, a load of 1.2N (contact pressure 0.4GPa), a linear velocity of 0.5mm/s, a reciprocating length of 3 mm, and a vacuum of  $5 \times 10^{-10}$  Torr. The results are shown in Fig. 4 (c), where the initial friction coefficient is 0.01, and after a few cycles, the friction coefficient decreases drastically to the 0.001 range. At some point, the friction coefficient appears negative, which may result from the noise being more significant than the signal from the sensor. Based on this, the authors concluded

that the MoS<sub>2</sub> films showed a friction disappearance phenomenon.

By comparing the HRTEM photographs of the pristine film and the abrasive chips (Fig. 4 (b)), it can be seen that the pristine MoS<sub>2</sub> film microcrystals show a long-range ordered edge-orientation structure with a disordered structure in the c-axis direction in the plane of the film, with grain sizes of about 7nm, and that there are defects in the MoS<sub>2</sub> film crystals such as planar curling, dislocations, and cavities. Finally, the surface was analyzed by XPS, AES, and RBS, pointing out that the films are pure, free of contamination, and consistent with the atomic stoichiometric ratio of MoS<sub>2</sub>.

HRTEM images of the abrasive chips demonstrate the friction-induced orientation of the MoS<sub>2</sub> grains at the contact interface, and the disappearance of the (002) diffraction ring indicates that the MoS<sub>2</sub> grains are oriented by friction, with their basal planes parallel to the sliding direction. In addition, locally magnified high-resolution images clearly show the presence of Moore's stripes due to the superposition of MoS<sub>2</sub> crystals and the rotation angle. Numerical diffractograms of both regions were obtained using an image

analyzer and the Fourier transform (EFT) algorithm, and it can be seen that regions 1 and 2 contain two different (001) orientations with mismatch angles of 16° and 29°, respectively(Fig. 5 (a,b,c)). Combined with the theory of structural superlubricity proposed by Hirano and Shinjo [32–34], the authors concluded that the MoS<sub>2</sub> film is reoriented during friction, which produces an incommensurate contact and frictional anisotropy, which is the source of superlubricity.

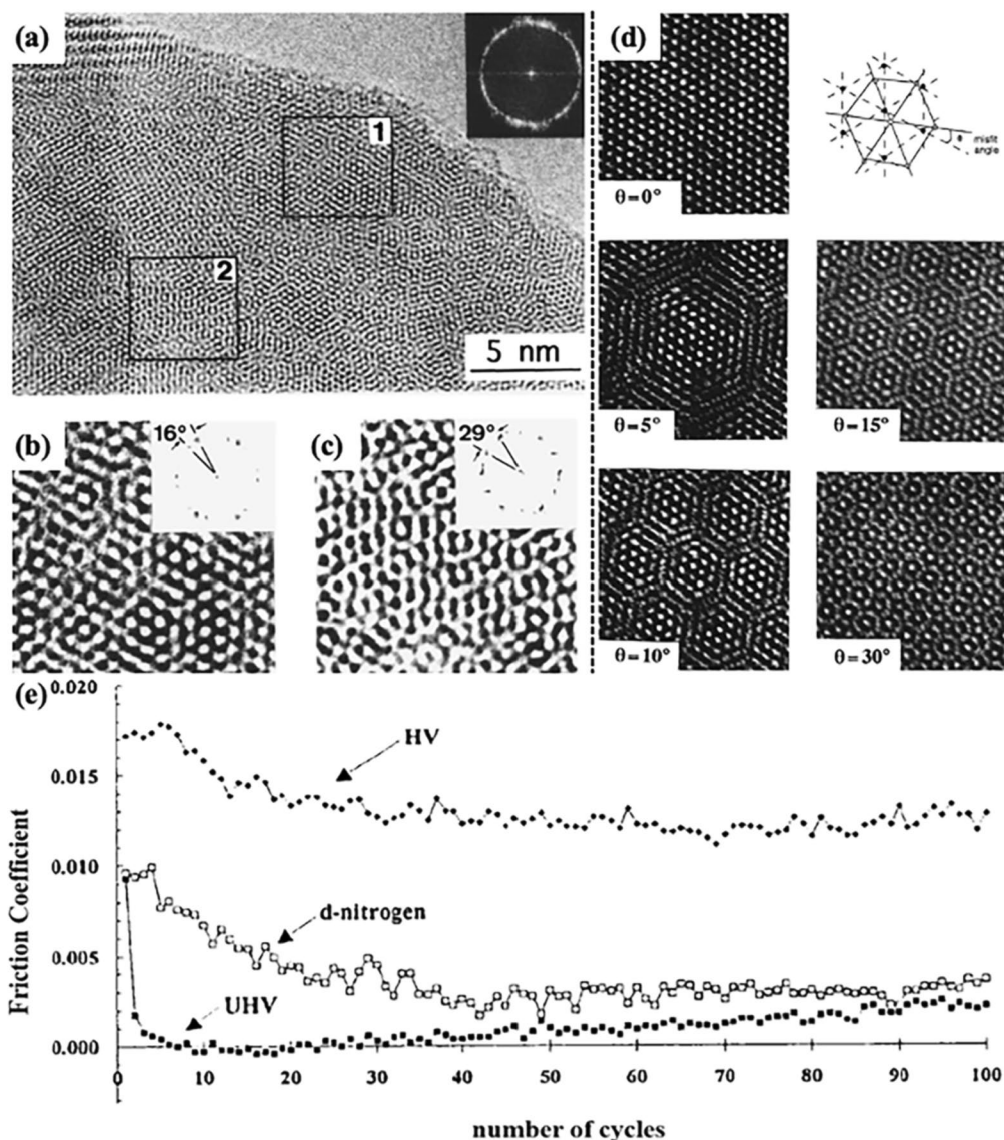


**Fig. 5** HRTEM photographs of MoS<sub>2</sub> abrasive chips (1 and 2 are enlarged images of region 1 (b) and region 2 (c) in (a), respectively; the rotation angles were obtained from the optical Fourier transform of the selected regions in the TEM images) [15], computational simulations showing the interference between two single-hexagonal lattices superposed at different rotation angles (d) (these interference images are very similar to the MoS<sub>2</sub> abrasive chip HRTEM image (a)) [15], friction coefficient curves of the pure MoS<sub>2</sub> films in different environments (e) [34, 35]. (a~d) reproduced from ref. 12. Copyright © 2007 Elsevier B.V; (e) reproduced from ref. 16. Copyright © 1993 Published by Elsevier B.V

To further investigate the effect of environment on the superlubricative properties of MoS<sub>2</sub> films, C. Donnet and J. M. Martin [15, 34, 35] comparatively investigated the effects of pure MoS<sub>2</sub> films in ultrahigh vacuum (UHV,  $5 \times 10^{-8} Pa$ ), high vacuum (HV,  $10^{-3} Pa$ ), pure nitrogen (N<sub>2</sub>,  $10^5 Pa$ , RH < 1%) and atmospheric ( $10^5 Pa$ , RH ~ 40%) environments, and the results of the tribological properties are shown in Fig. 5 (e). The film friction coefficients in air ranged between 0.15 and 0.20 (not shown in the figure). In HV, the coefficient of friction decreased to an ultra-low state and remained between 0.015 and 0.018. In dry N<sub>2</sub>, the friction coefficient reaches a super-lubricated state. Finally, it stabilizes at 0.003, while in UHV, the films have the lowest friction coefficients, ranging from 0.001 to 0.002, and even appear to have a state where friction disappears completely. It suggests that contaminants in the environment have an essential effect on superlubricity, causing an increase in the coefficient of friction even in dry N<sub>2</sub>, which may contain shallow oxygen impurities. In HV and atmospheric environments, the increase in contaminants leads to the loss of superlubricative properties of the films.

Based on the above studies, C. Donnet and J. M. Martin suggest that superlubricity is related to four critical processes: (1) the films are prepared in ultrahigh vacuum, and friction is carried out in situ; (2) sliding friction between the counterpart ball and the film and a MoS<sub>2</sub> transfer film is formed on the surface of the counterpart ball; (3) the MoS<sub>2</sub> films (both pristine and transferred) undergo a sliding orientation and crystalline orientation; (4) another crystal orientation mechanism is introduced during friction: friction induces microcrystals to rotate around the c-axis, producing lattice mismatch angles and incommensurate contacts [15, 31].

The theory of Hirano and Shinjo of structural superlubricity [32–34] suggests that superlubricity is related to the atomic interlocking of friction, which occurs when the sum of the forces acting on each moving atom vanishes concerning the whole system. Their theoretical calculations show that friction disappears when two ideal crystal planes undergo an incommensurate contact motion. Therefore, the realization of superlubricity between two crystal planes requires the fulfillment of three conditions: (1) atomically clean surfaces, (2) weak interaction forces between interacting atoms, (3) incommensurate atomic lattice contact between the two crystal planes.

Since the films were prepared in ultrahigh vacuum and the ultrahigh vacuum friction was performed in situ, the films were not exposed to any contaminated environment. Therefore, the atomically clean surface required by condition (1) is satisfied by the oxygen-free MoS<sub>2</sub> films prepared under ultrahigh vacuum condition. When

oxygen is present, O entering the basal plane replaces the S atoms. Since the Mo-O bond is shorter than the Mo-S bond, atomic-level defects are created, causing an energy barrier that will increase the coefficient of friction [36]. For pure MoS<sub>2</sub> films, there are weak van der Waals forces between the S-Mo-S layers in the crystal structure, which can satisfy condition (2) weak interaction requirement. Even if the prepared pristine film presents a disordered structure, the shear force during the friction process can make the film re-crystallized and oriented to form a (002) base surface parallel to the sliding direction. Moreover, the surface of the counterpart ball also forms an ordered transfer film with (002) basal plane orientation. Hence, the friction interface occurs between the MoS<sub>2</sub> (002) basal plane layers, and there are only weak van der Waals force interactions between the interacting atoms. Also, solid chemical reactions and interactions are avoided when friction is performed in an ultrahigh vacuum and N<sub>2</sub>.

The abrasive chip HRTEM analysis shows the presence of MoS<sub>2</sub> crystal superposition and rotation angles of 16° and 29° at the friction interface, which satisfies condition (3) incommensurate atomic contact. However, theoretical calculations show that for two 2H-MoS<sub>2</sub> crystal sliding surfaces, incommensurate contact is obtained at a mismatch angle of 30° (e.g., Fig. 5 (d)), which achieves frictional anisotropy. However, Sokoloff calculated [37] that for incommensurate contact interfaces, the friction (or dissipative stress) is  $10^{13}$  times smaller than for metric interfaces. Thus, once the interface approaches the mismatch angle, the friction is substantially reduced by several orders of magnitude. Moreover, it is not necessary to have a precise mismatch angle (e.g., 30° for MoS<sub>2</sub>) to achieve an extremely low friction state, and even minimal rotation angles are sufficient to reduce friction substantially [15].

The pioneering work of C. Donnet and J.M. Martin et al. discovered the phenomenon of superlubricity in pure MoS<sub>2</sub> films and proposed a superlubricity mechanism. However, there is a significant gap with practical applications due to the need for high vacuum in-situ preparation, in-situ friction, and in-situ analysis.

### 3.2 Superlubricity of MoS<sub>2</sub> films with special nanostructure

In 2000, Chhowalla [16] prepared fullerene MoS<sub>2</sub> nanofilms by localized high-voltage arc discharge, which possess friction coefficients less than 0.01 and exhibit superlubricity properties in both dry N<sub>2</sub> and humid air (RH=45%). Moreover, the low-temperature preparation process of this kind of fullerene MoS<sub>2</sub> nanofilm makes it easy to deposit the film on the surface of automobiles, tools, disks, and other parts. Hence, the MoS<sub>2</sub>



superlubricity film has the prospect of engineering applications.

The Fullerene-MoS<sub>2</sub> nanofilm preparation process is as follows: through the introduction of N<sub>2</sub> in the MoS<sub>2</sub> target 1mm holes to generate localized high pressure, in the high-pressure N<sub>2</sub> localized area ignited arc (75A and 22V), ablation of MoS<sub>2</sub> target, the deposition of films on the surface of the substrate. 440C stainless steel substrate from the target material of 20cm, the pressure is maintained at 10mTorr, the deposition temperature of 200°C or less. The MoS<sub>2</sub> films were 1.2 ± 0.1µm thick, with a hardness of 10GPa and a bonding force of 25N.

Fullerene-MoS<sub>2</sub> nanofilms were prepared by localized high-voltage arc discharge, and circular nanoparticles with a diameter of 30nm and curved S-Mo-S planes were easily seen (Fig. 6 (a)), indicating the formation of well-shaped hollow fullerene "onion" MoS<sub>2</sub> nanoparticles in

the films. The key mechanism for the formation of nanoparticles is the bending and rearrangement of the basal planes. Mo or S undergoes substitution by collision with energetic ions in the arc plasma, leading to atomic rearrangement to maintain electrical neutrality. In contrast, MoS<sub>2</sub> films prepared by conventional sputtering are mostly amorphous with only localized and incomplete hexagonal bending structures (Fig. 6 (b)).

The tribological properties of fullerene MoS<sub>2</sub> nanofilms, conventional sputtered MoS<sub>2</sub> films in a humid (RH45%) atmosphere, and N<sub>2</sub> were investigated comparatively by ball-disk friction tester (test conditions: counterpart ball of Φ7mm 440C steel balls, load 10N, speed 50cm/s), and the results are shown in Fig. 6 (c). The fullerene MoS<sub>2</sub> nanofilms showed a super-lubricating friction coefficient of 0.006 in N<sub>2</sub>, and even under an atmosphere of RH45%, they still had a friction coefficient

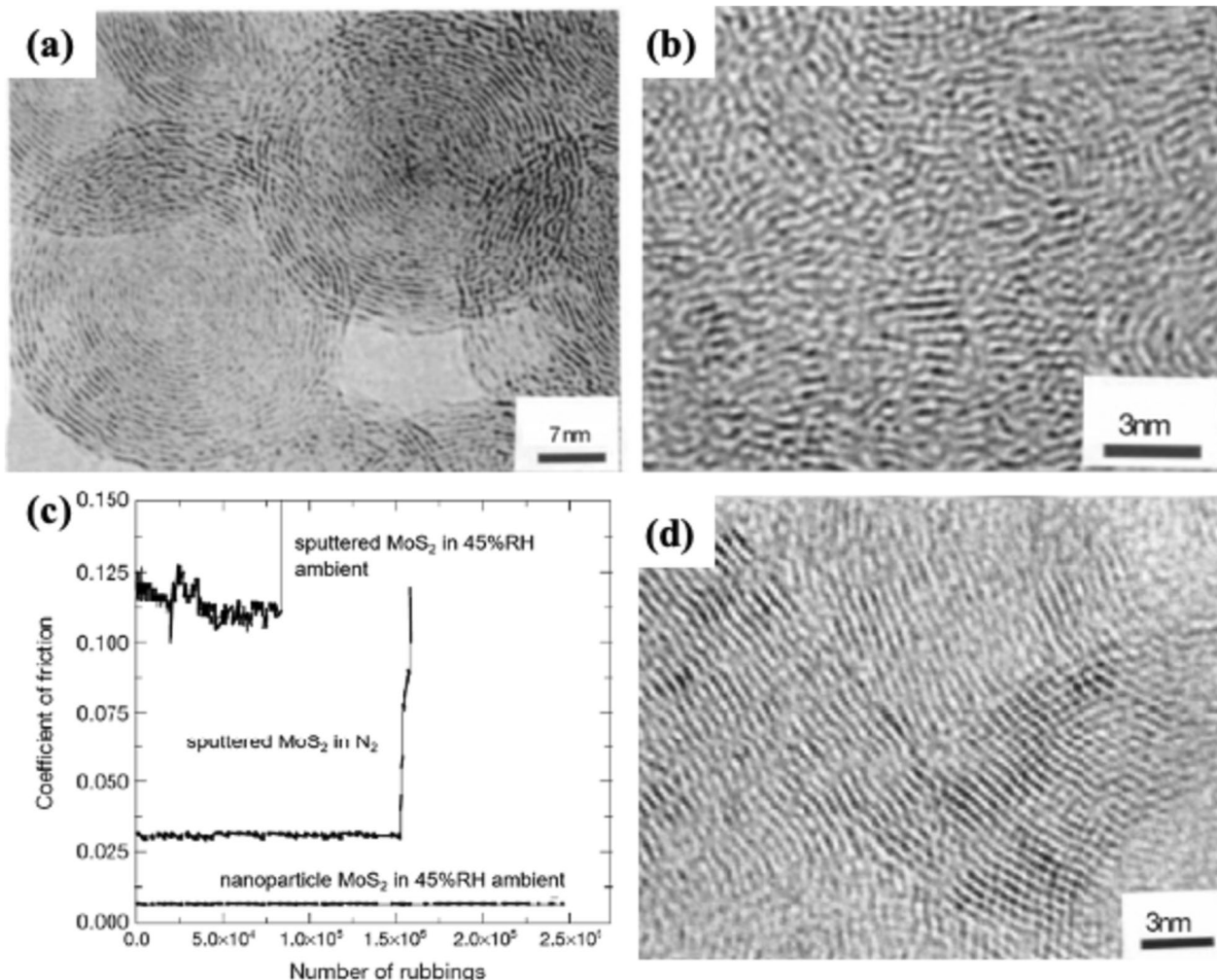


**Fig. 6** HRTEM images of (a) fullerene-like MoS<sub>2</sub> nanofilms and (b) conventionally sputtered MoS<sub>2</sub> films, friction coefficient profiles of different MoS<sub>2</sub> films in different environments (c), and HRTEM images of MoS<sub>2</sub> nanofilm abrasive chips after 2.4 × 10<sup>5</sup> cycles in RH45% atmosphere (d) [16]. (a~d) reproduced from ref. 20. Copyright © 2000 Macmillan Magazines Ltd



of 0.008 ~ 0.01 and a very low wear rate of  $1 \times 10^{-11} \text{mm}^3/\text{Nm}$ . For conventional sputtered MoS<sub>2</sub> films, the coefficient of friction is about 0.03 in N<sub>2</sub> and higher than 0.10 in the RH45% atmosphere.

Figure 6 (d) shows the HRTEM image of abrasive chips of fullerene MoS<sub>2</sub> nanofilms after  $2.4 \times 10^5$  cycles in a RH45% atmosphere. Observations show that there are almost no closed circular nanoparticles. However, the bent hexagonal lattice remains intact, suggesting that the large fullerene nanoparticles fragment into smaller irregularly shaped bent microcrystals under loaded friction conditions.

The authors concluded that in addition to the traditional lubrication mechanisms such as easy shear lamellar structure, uniform transfer film formation, and intergranular slip, the presence of curved hexagonal planes in the fullerene MoS<sub>2</sub> nanofilms, the hexagonal planar structure reduces the number of dangling bonds exposed at the edges of the planes and reduces the oxidation of the Mo atoms, which significantly enhances the stability properties of the films in humid environments, thus contributing to the maintenance of the lamellar structure and the ultra-low friction for a more extended period.

Kaiming Hou [38] prepared stacked loose MoS<sub>2</sub> nanosheet coatings using a hydrothermal method, and when friction was performed in vacuum (test conditions: vacuum at  $3.5 \times 10^{-3} \text{Pa}$ , mating pair of  $\Phi 3 \text{mm}$  AISI 52100 steel balls, and a load of 0.5 ~ 2N), it was found that under reciprocating shear stress-induced in-situ friction interface it was found that under reciprocal shear stress-induced in-situ formation of spherical MoS<sub>2</sub> nanoparticles with cabbage-like structure and friction coefficients ranging from 0.004 to 0.006 at the friction interface, the superlubricity state was easily realized. The authors concluded that spherical MoS<sub>2</sub> nanoparticles reduce friction to realize superlubricity through the following four aspects:

(1) Spherical MoS<sub>2</sub> nanoparticles roll under low stress and slide under high stress, and this sliding/rolling mechanism is considered the key to reducing friction; (2) The curved structure endows mechanical strength and elasticity to spherical MoS<sub>2</sub> nanoparticles, which can buffer the loading stresses; (3) Reducing the interfacial contact area will weaken the interaction between the film and the counterpart ball; (4) The incommensurate contact between the spherical MoS<sub>2</sub> nanoparticles and the MoS<sub>2</sub> film leads to the minimum sliding resistance.

### 3.3 Superlubricity of MoS<sub>2</sub> composite films

The earliest studies concluded that introducing contaminants (e.g., O, C, and other doping elements) into MoS<sub>2</sub> would lead to elevated friction coefficients and superlubricity failure [1, 15, 31, 35, 39]. However, in practical

applications, contamination is inevitable. On the one hand, the residual gases (e.g., O, H<sub>2</sub>O, C) in the vacuum chamber during film preparation are doped into the MoS<sub>2</sub> films. As a result, most vacuum-deposited MoS<sub>2</sub> film structures contain a certain amount of O (10 ~ 20 at.%). On the other hand, the applications of MoS<sub>2</sub> films are becoming more and more widespread, and researchers want to develop MoS<sub>2</sub> films that can be adapted to different environments. Even in space applications, the MoS<sub>2</sub> film has to go through ground installation, testing, and storage before launch, which requires the MoS<sub>2</sub> film to adapt to the humid ground environment. Therefore, developing adaptive (chameleon) lubricated films by preparing multi-composite MoS<sub>2</sub> films by doping various metals, nonmetals, oxides, etc., has received extensive attention and great success from researchers [40]. Whether and how the MoS<sub>2</sub> films can maintain and realize the superlubricative performance after doping is also the attention focus of the researcher.

There is a synergistic effect between graphitic carbon and MoS<sub>2</sub> [41] and Sb<sub>2</sub>O<sub>3</sub> and MoS<sub>2</sub> [42], which can improve the moisture and oxidation resistance of MoS<sub>2</sub> films. Therefore, Zabinski [43] prepared MoS<sub>2</sub>/Sb<sub>2</sub>O<sub>3</sub>/C composite films using a mixture of MoS<sub>2</sub>, graphite, and Sb<sub>2</sub>O<sub>3</sub> powders (40:40:20 wt.%) by rubbing on 440C steel and examined the tribological properties of the films in the air (RH ~ 50%), dry N<sub>2</sub>, and in high vacuum ( $10^{-8} \text{Torr}$ ). The test conditions are a load of 100 g, a rotational speed of 200 rpm, and mated with  $\Phi 6.35 \text{mm}$  440C steel balls. The results show that the MoS<sub>2</sub>/Sb<sub>2</sub>O<sub>3</sub>/C composite film has a lower coefficient of friction and a longer wear life than the pure MoS<sub>2</sub> film in humid atmospheric conditions. Especially in dry N<sub>2</sub> and high vacuum, the friction coefficients of the MoS<sub>2</sub>/Sb<sub>2</sub>O<sub>3</sub>/C composite films were less than 0.01, which reached the super-lubricated state. In dry N<sub>2</sub>, the friction coefficient of the film was maintained at 0.008 after  $10^7$  cycles, and the film did not fail. During friction, MoS<sub>2</sub> forms a (002) layered, dense stacking structure parallel to the sliding direction in the most superficial layer of the friction interface, which is oxidation-resistant and inert. It has a smooth crystalline surface, thus achieving superlubricity. In the subsurface layer of the friction interface, a Sb<sub>2</sub>O<sub>3</sub> dominated particle layer is formed, which effectively inhibits the crack formation and extension and plays a certain supporting role, which is very important for improving life.

Li Hongxuan [44] prepared MoS<sub>2</sub>/a-C:H composite films by reactive magnetron sputtering of MoS<sub>2</sub> target and graphite target with CH<sub>4</sub> and Ar and investigated the tribological properties of the films under vacuum ( $5 \times 10^{-3} \text{Pa}$ ) (load of 5N, rotational speed of 300 rpm, and mated with a pair of  $\Phi 6 \text{mm}$  GCr15 steel balls). It was found that the MoS<sub>2</sub>/a-C:H film prepared at Ar/

CH<sub>4</sub>=105/5 had a typical nanocrystalline/amorphous composite structure, with 10nm MoS<sub>2</sub> nanocrystals embedded in an amorphous carbon network structure and that the film had superlubricity friction coefficient of 0.002 in a vacuum, but the superlubricity mechanism was not discussed.

Based on this work, the authors also prepared MoS<sub>2</sub>-C composite films using co-sputtered MoS<sub>2</sub> and graphite targets [45], which had a dense structure with a uniformly distributed MoS<sub>2</sub> (002) lattice. The C, Mo, and S contents were 56at.%, 12at.%, and 32at.%, respectively. The vacuum friction results show that (vacuum degree 5×10<sup>-3</sup>Pa, reciprocating sliding distance 5mm, linear velocity 10cm/s, load 10N, mated with a pair of Φ6mm GCr15 steel balls), the friction coefficient is reduced to less than 0.01 after a short period of grinding. The average friction coefficients of the three repetitions of the test are 0.0068, 0.0060, and 0.0089, which have reached the engineering superlubricative condition. The friction coefficient is stable and repeatable (Fig. 7 (f)).

HRTEM analysis of the film wear track on MoS<sub>2</sub>-C films and the counterpart ball wear scar revealed that a friction interface layer with a thickness of about 20-30nm was formed on the surface of the wear track. A large number of ordered MoS<sub>2</sub> (002) lattices parallel to the sliding direction existed within the friction interface layer (Fig. 7 (a,b)). A dense transfer film with a thickness of about 10nm was formed on the surface of the counterpart ball wear scar after friction, which was analyzed and shown to be amorphous carbon (Fig. 7 (c,d,e)). Therefore, the authors concluded that during the friction between the MoS<sub>2</sub>-C heterogeneous composite film and the counterpart ball, carbon was selectively transferred to the surface of the counterpart ball to form a dense amorphous carbon transfer film. A layer of parallel ordered MoS<sub>2</sub> crystals of 20~30nm was formed on the surface of the grinding spot of the MoS<sub>2</sub>-C composite film, and friction occurred between the amorphous carbon and the MoS<sub>2</sub> crystals. There is a lattice constant mismatch between the disordered

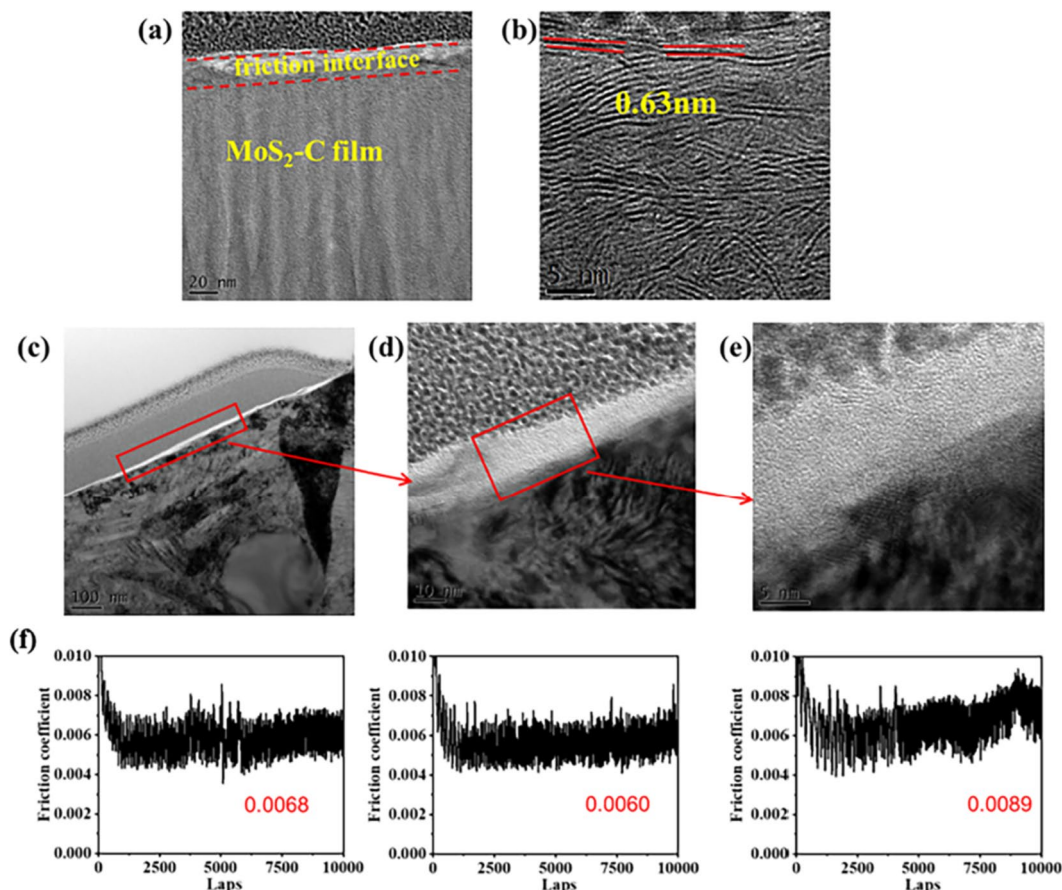


**Fig. 7** Cross-sectional FIB-HRTEM images of wear track on MoS<sub>2</sub>-C films and the counterpart ball wear scar after friction in vacuum, HRTEM images of wear track cross-section (a) (b), TEM images of wear scar cross-section (c~e) [45], Friction curves (three repetitions of the test) of MoS<sub>2</sub>-C films under vacuum (f) [45]. (a~f) reproduced from ref. 27. Copyright © 2023 Tribology

amorphous material and the ordered crystalline material, and the heterogeneous structure composed of amorphous and crystalline can form an incommensurate contact to reduce the friction and realize the superlubricity on the macroscopic scale.

MoS<sub>2</sub>/Sb<sub>2</sub>O<sub>3</sub>/Au composite films have been widely studied and applied [46–50], with typical contents of 82%MoS<sub>2</sub>, 11%Sb<sub>2</sub>O<sub>3</sub>, and 7%Au molar content. Scharf prepared 1μm thick MoS<sub>2</sub>/Sb<sub>2</sub>O<sub>3</sub>/Au composite films on 440C steel using magnetron sputtering [49] in drying N<sub>2</sub>, and the friction coefficient was 0.006~0.007 after a short friction coefficients of 0.006~0.007 after abrasion. Therefore, adding Au and Sb<sub>2</sub>O<sub>3</sub> to MoS<sub>2</sub> does not adversely affect its superlubricitive behavior in dry N<sub>2</sub>. HRTEM analysis of the wear track surfaces showed that friction led to an amorphous-to-crystalline transition of MoS<sub>2</sub>, with the (002) basal planes aligned parallel to the sliding direction. The transfer film on the surface of counterpart ball also consists of the (002) basal plane orientation of MoS<sub>2</sub> so that the friction is mainly sliding at

the "base-to-base" interface of the self-mating pair, thus reducing friction and wear.

Recently, the results of Yin [14] showed that MoS<sub>2</sub>-Ag multilayer composite films exhibit superlubricitive properties at low temperatures. The authors prepared Ag-doped MoS<sub>2</sub> composite multilayer films on steel substrates using magnetron sputtering and ion beam-assisted deposition techniques, with a composite structure of Ag nanoparticles distributed in a MoS<sub>2</sub> structure and a multilayer structure with alternating Mo-rich and MoS<sub>2</sub> layers (the thickness of Mo-rich layer is 3~4nm). The tribological properties of the composite multilayer films were investigated at different temperatures in a lightly loaded (1N) liquid helium atmosphere and a low temperature of 170K in a heavily loaded (10N) liquid nitrogen atmosphere.

Figure 8 (a) shows the friction results of the films tested at different temperatures (10 temperature points). The friction curves show that the friction coefficients at all temperature points from 20 to 295K satisfy the

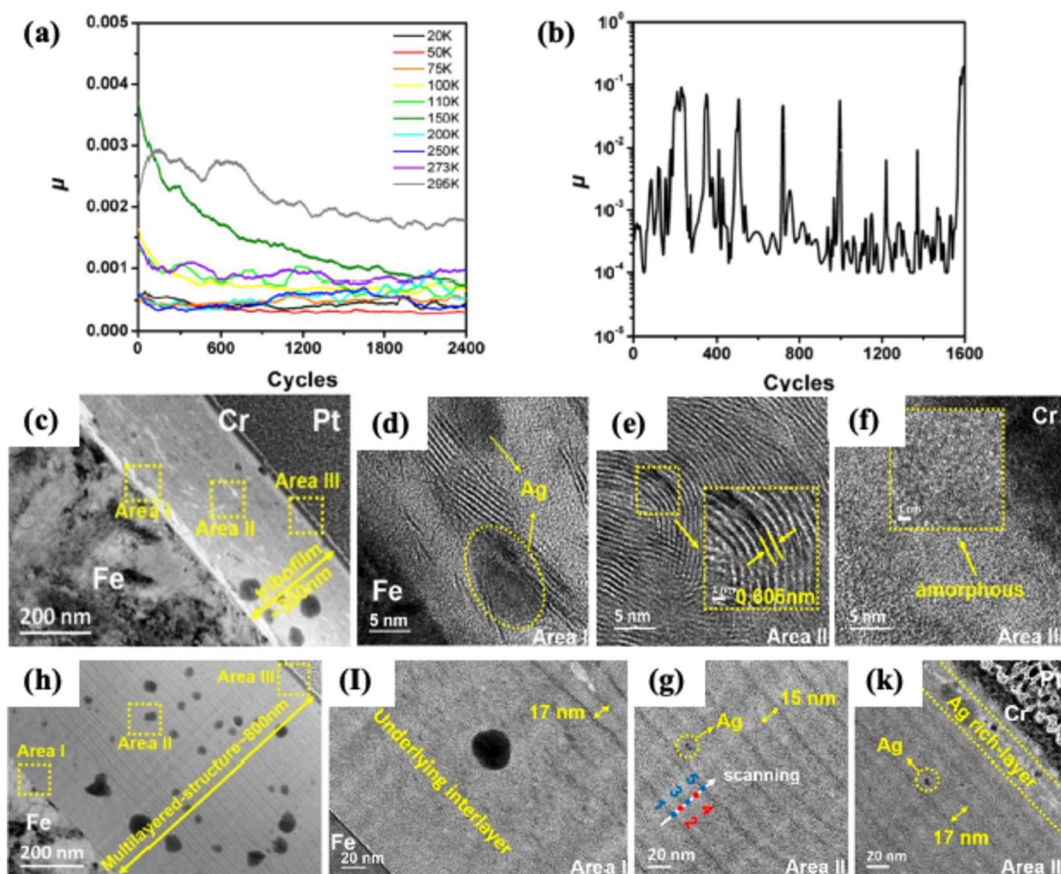


**Fig. 8** Friction coefficient curves of MoS<sub>2</sub>-Ag composite multilayer films mated with steel balls (a) Liquid helium, 1 N load, different temperatures (b) Liquid nitrogen, 10N load, 170K cryogenic temperature, HRTEM analysis of counterpart ball wear scar (c~f) and wear track on MoS<sub>2</sub>-Ag films (h~k) [53] (c) Overall morphology of the transfer film, (d) Bottom region, (e) Middle region, (f) Outermost layer, (h) Overall morphology of the film, (i) Bottom region, (g) Middle region, (k) Outermost layer [14]. (a~k) reproduced from ref. 33. Copyright © 2021 American Chemical Society



superlubricative state ( $\mu \leq 0.01$ ). The lowest friction coefficients were found from 20 to 50K, reaching 0.0004–0.0005, which the authors consider the lowest friction coefficient values in macroscopically lubricated systems to date. The post-friction Raman spectra at 20K are similar to those of pristine films, which suggests that low temperatures are conducive to protecting the MoS<sub>2</sub> microcrystals to achieve superlubricity. 150K and 295K friction coefficients were relatively high, around 0.001~0.002, which may be related to surface adsorption. However, previous studies have found that the friction coefficients of MoS<sub>2</sub> films are generally elevated at low temperatures, and scholars have suggested that the friction coefficients are expected to increase by at least a factor of two when MoS<sub>2</sub> films are used in ultralow-temperature instrumentation [25, 48, 51, 52]. Therefore, further studies on the tribological properties of MoS<sub>2</sub> films at low temperatures are still needed.

Figure 8 (b) shows the friction profile of the film at 170K under a heavy load of 10N. The composite multilayer film can withstand pressures above 2GPa and maintains an average coefficient of friction of less than 0.001 at 170K. The friction profile of the film at 170K under a heavy load of 10N. During the sliding process, the MoS<sub>2</sub> nanosheets are continuously consumed by the friction on the contact surface. At the same time, Ag nanoparticles embedded in the membrane gradually aggregated to form larger Ag nanoparticles in situ (Fig. 8 (h~k)) or were removed together with exfoliated MoS<sub>2</sub> nanosheets and transferred to the counterpart ball surface (Fig. 8 (c~f)). As a result, the shear interface shifted from between the bare sphere and the MoS<sub>2</sub> nanosheets to between the friction film (composed of MoS<sub>2</sub> nanoparticles and Ag nanoparticles) and Ag nanoparticles. These soft nanomaterials, such as Ag nanoparticles and MoS<sub>2</sub> nanosheets, could reduce friction and wear to a very low levels compared to the friction interface between bare spheres and pristine MoS<sub>2</sub> films. In addition to the formation of shear-prone interfaces, another essential factor in achieving superlubricity is the multilayer structure. The film comprises Mo-rich layers and MoS<sub>2</sub> nanosheets distributed between them (Fig. 8 (h~k)). Upon contact, the sliding behavior of the MoS<sub>2</sub> nanosheets is limited by the Mo-rich layers between them, which drives most of the MoS<sub>2</sub> nanosheets to slide in the direction of the film surface. Therefore, the above two synergistic effects are the key to realizing the superlubricity of multilayer composite films at low temperatures.

Guomin Yu [54] found that certain content of O<sub>2</sub> can reduce the friction coefficient between MoS<sub>2</sub>/H-DLC films and Al<sub>2</sub>O<sub>3</sub> counterpart ball and realize superlubricity. The authors first prepared H-DLC films in CH<sub>4</sub> and H<sub>2</sub> plasma using the PECVD technique. Then MoS<sub>2</sub>

flakes were dispersed in ethanol and sprayed onto the surface of H-DLC films, and MoS<sub>2</sub>/H-DLC composite films were formed after ethanol evaporation and drying. The tribological properties of the composite films with Al<sub>2</sub>O<sub>3</sub> spheres in different atmospheres were investigated.

In Ar, the friction coefficient of the composite films increased gradually with time and was less than 0.01 during the first 300s. In N<sub>2</sub>, the friction coefficient was 0.005 during the initial 60s of friction but then increased to 0.025 during stabilization. At the same time, in O<sub>2</sub>, the friction coefficients were low as 0.003~0.005 during the whole friction period.

In order to further investigate the role of O<sub>2</sub> in superlubricity, the authors pass O<sub>2</sub> into Ar and N<sub>2</sub> according to a specific ratio, respectively, and found that the friction coefficients of the composite films can be stabilized at 0.002–0.003 for a long time when the O<sub>2</sub> volume content reaches 16.7% in both Ar and N<sub>2</sub>, achieving stable superlubricity. Based on the experimental results and first-principle calculations, the authors concluded that in Ar and N<sub>2</sub>, the short-time superlubricity was attributed to the transfer film formed on the Al<sub>2</sub>O<sub>3</sub> spheres at the initial friction stage. However, the transfer film could not be stabilized on the surface of Al<sub>2</sub>O<sub>3</sub> spheres for an extended period in these inert atmospheres, leading to superlubricity failure. Instead, O atoms can bond with Mo, S, and Al atoms to form bridge bonds that stabilize the MoS<sub>2</sub> transfer film on the Al<sub>2</sub>O<sub>3</sub> ball surface. The friction occurs between the MoS<sub>2</sub> transfer film and H-DLC, forming an incommensurate contact at the interface, leading to stable superlubricity.

For over 30 years, pure MoS<sub>2</sub> and MoS<sub>2</sub> films doped with various elements have achieved superlubricity under high vacuum, dry N<sub>2</sub>, O<sub>2</sub>, and moist air. However, achieving universal superlubricity is still an active research topic. The combination of homogeneous transfer film formation and retention, (002) basal plane ordered orientation and intercrystalline shear, intergranular slip, incommensurate contact, and weak chemical interactions are possible mechanisms for the superlubricity of MoS<sub>2</sub> films.

### 3.4 Key factors in achieving the superlubricity of MoS<sub>2</sub> films

- (1) Uniform transfer film formation and retention. In the process of MoS<sub>2</sub> film friction, MoS<sub>2</sub> and counterpart materials have good adhesion and form a uniform and dense transfer film on the surface of the counterpart. The transfer film structure is (002) ordered base plane parallel to the sliding direction, which is widely recognized by the researchers of the MoS<sub>2</sub> low friction mechanism [1, 25]. The interfa-

cial properties and friction conditions determine the transfer film, and maintaining the stable existence of the transfer film is one of the controlling conditions for the low-friction and long life of MoS<sub>2</sub> films. Therefore, it is necessary to deeply analyze the transfer film formation regularity at the friction interface.

- (2) Ordered (002) basal plane orientation and intercrystalline shear. It has long been recognized that when MoS<sub>2</sub> films slide relative to each other, the MoS<sub>2</sub> at the frictional interface reorients to form an ordered (002) basal plane parallel to the sliding direction [18, 25, 31]. The intercrystalline easy shear in the basal plane direction (weak van der Waals forces connect layers) is believed to be the main reason for the very low friction coefficient of MoS<sub>2</sub>. Two features characterize the ordered orientation of the basal plane. One is independent of whether the original film is crystalline or not. It has been demonstrated that basal-plane-oriented, prismatic-plane-oriented, and fully amorphous MoS<sub>2</sub> films can undergo (002) basal plane reorientation under friction and parallel to the sliding direction, as shown in Fig. 9 [18]. Secondly, the ordered orientation mainly occurs at the sliding interface. It does not affect the overall structure of the film, depend-

ing on the friction conditions, and the thickness of the ordered orientation is probably in the order of 10nm.

- (3) Intergranular slip and incommensurate contact. Intercrystalline slip has been used to explain the superlubricity behavior of MoS<sub>2</sub> because friction is mainly intergranular sliding of MoS<sub>2</sub> "base to base" due to the formation of ordered transfer films and the ordered orientation of the film surface (002) basal planes [18, 49]. C. Donnet and J. M. Martin et al [1, 15, 31] found that MoS<sub>2</sub> crystals in abrasive chips existed at an angle of rotation, realizing incommensurate contact and frictional anisotropy, with a significant reduction in friction to achieve superlubricity. Recent studies have shown that heterostructures of MoS<sub>2</sub> and graphene [2, 55, 56] and MoS<sub>2</sub> and amorphous carbon [45, 54] can form incommensurate contact and realize superlubricity.
- (4) Weak chemical interactions. Chemical bonding interactions at the friction interface cause strong adhesion, sticking, and high friction. The O element often exists in MoS<sub>2</sub> films as molybdenum oxide or as substituted S atoms, causing lattice distortions and defects [36]. In addition, water vapor in the air disrupts the shear-prone lamellar structure and oxidizes the edge sites, severely increasing the

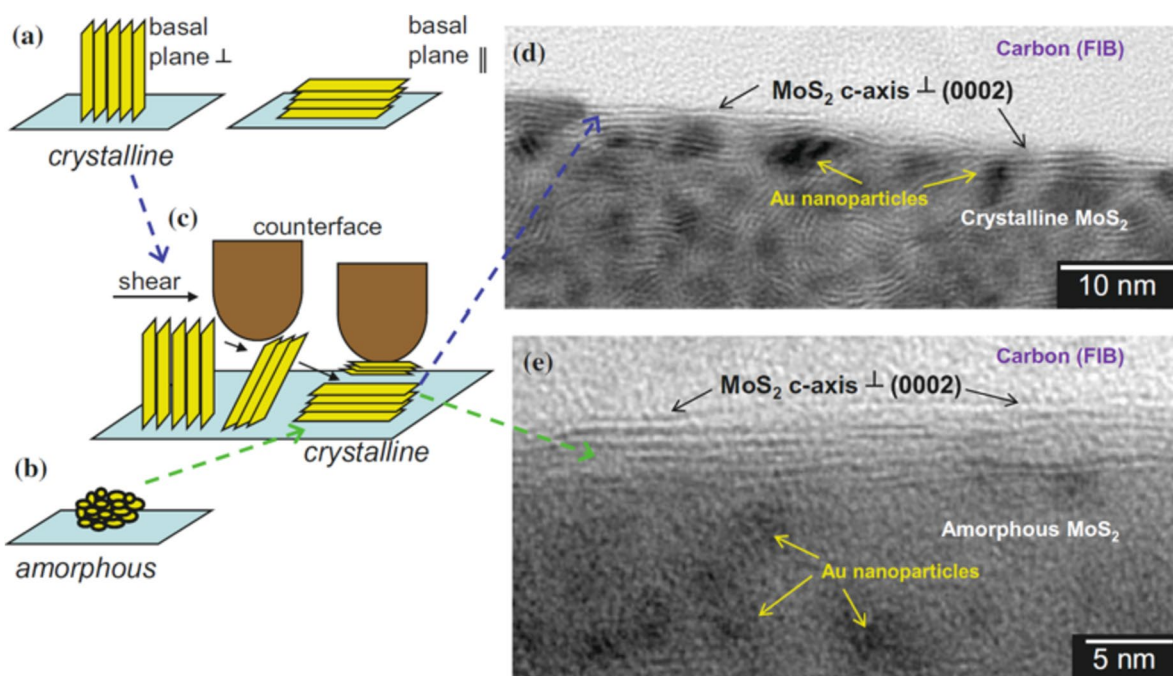


**Fig. 9** Schematic of friction-induced crystallographic orientation of MoS<sub>2</sub> films [18] (a) Edge-oriented and basal oriented films (b) Amorphous structured films (c) Schematic of friction-induced orientation (d,e) Interfacial TEM analysis (a-c-d) Processes of reorientation of edge-oriented or basal oriented films to achieve low friction (b-c-e) Amorphous to crystalline transition to achieve low friction. (a~e) reproduced from ref. 3. Copyright ©2012 J Mater Sci

sliding resistance [57–59]. Modulation of weak chemical interactions at the interface is one way to reduce friction. Methods to reduce weak chemical interactions include reducing contaminants such as oxygen and water in MoS<sub>2</sub> films, controlling the MoS<sub>2</sub> structure to reduce active sites such as prismatic dangling bonds and defects, and providing an inert environment. For example, MoS<sub>2</sub> often exhibits superlubricative properties in ultra-high vacuum and dry N<sub>2</sub> because the vacuum and N<sub>2</sub> provide an environment for weak chemical interactions.

## 4 Important effects on the superlubricity of MoS<sub>2</sub> films

### 4.1 Effects of oxygen and water

The tribological properties of MoS<sub>2</sub> films are sensitive to environmental conditions. In general, MoS<sub>2</sub> films exhibit ultra-low friction and wear in high vacuum and dry inert atmosphere. In the presence of O<sub>2</sub> and water, the coefficient of friction rises and wear increases. In 1953, Peterson and Johnson [60] first investigated the dependence of lubrication properties of MoS<sub>2</sub> films on humidity, and the results showed that MoS<sub>2</sub> friction first increases and then decreases as the humidity increases to 65%. Researchers began to emphasize and extensively study the effects of O<sub>2</sub> and water on the tribological properties of MoS<sub>2</sub> films.

Due to the small amount of water and O<sub>2</sub> remaining in the vacuum chamber during sputtering and the fact that the films will inevitably be exposed to atmospheric conditions, a certain amount of O (10~20at.%) exists in all MoS<sub>2</sub> films, and the doping of O affects the crystal structure, orientation, and film morphology.

According to XRD and EXAFS analyses [15, 53, 61], the effect of increased O content in MoS<sub>2</sub> films is threefold: (1) an increase in the MoS<sub>2-x</sub>O<sub>x</sub> phase (the same structure as MoS<sub>2</sub>, with O substituting for S); (2) an increase in *x* in MoS<sub>2-x</sub>O<sub>x</sub> and (3) a decrease in the long-range and short-range ordered structures. O replaces S to form the MoS<sub>2-x</sub>O<sub>x</sub> phase, which causes the (100) lattice to shrink and the microcrystalline size to decrease due to the shorter Mo–O bond than the Mo–S bond, resulting in a highly dense film, which is favorable for improving the load-bearing capacity [53]. In addition, the MoS<sub>2-x</sub>O<sub>x</sub> microcrystals, although contracting in the (100) direction, expand in the (002) basal plane [40, 62], and the expansion of the basal distance leads to a reduction of the shear strength between the S–Mo–S sandwich layers in the microcrystals. Thus the MoS<sub>2-x</sub>O<sub>x</sub> phase also has a low coefficient of friction [63]. It has been found [64] that the friction coefficient of sputter-deposited MoS<sub>2</sub> films decreases with increasing O<sub>2</sub> partial pressure in a vacuum.

Molybdenum oxide (MoO<sub>*y*</sub>) is formed when the O content increases further. MoO<sub>*y*</sub> hard particles cause a higher coefficient of friction and wear rate during friction. Atmospheric O<sub>2</sub> molecules have a small effect on the tribological properties of MoS<sub>2</sub> films at room temperature [65]. However, at high temperatures, they oxidize the edge active sites and grain boundaries, generating MoO<sub>2</sub> and MoO<sub>3</sub>, which destroys the shear-prone lamellar slip structure of MoS<sub>2</sub>, leading to high friction and wear [66, 67]. Increasing temperature increases the oxidation rate, and tribological properties deteriorate significantly.

MoS<sub>2</sub> films with highly ordered basal plane orientation exhibit higher oxidation resistance than amorphous MoS<sub>2</sub> films [68]. The basal plane-oriented MoS<sub>2</sub> films have only inert S atoms exposed in the outermost layer and thus are highly chemically inert, limiting oxidation to the most superficial molecular layer. In contrast, MoS<sub>2</sub> films with amorphous structures are eroded by O<sub>2</sub> to a much greater depth than basal plane-oriented MoS<sub>2</sub> films, resulting in a more extended wear period and lower friction life. It suggests that controlling the deposition technique, reducing the density of edge active sites, and preparing a highly ordered structure with basal plane orientation reduce the oxidation of MoS<sub>2</sub> films and thus minimize the environmental sensitivity of the tribological properties of MoS<sub>2</sub> films.

AO is abundant in LEO space (with an atomic flux density of 10<sup>13</sup>~10<sup>15</sup> atoms·cm<sup>-2</sup>·s<sup>-1</sup> and kinetic energy of 5eV). The effects of AO on the tribological properties of MoS<sub>2</sub> films have been widely studied at home and abroad [69–71], which showed that the loss of S atoms and oxidation of Mo atoms during prolonged irradiation of AO destroyed the interlayer lubrication structure of MoS<sub>2</sub>, leading to degradation of lubrication properties of MoS<sub>2</sub> films. AO flux density, irradiation time, and the wear volume and friction coefficient of film are positively correlated [69].

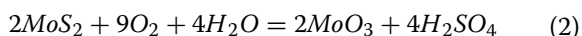
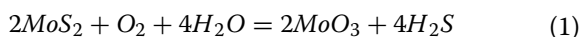
Oxidation of the film surface increases the coefficient of friction. In contrast, when friction occurs in a high vacuum or a dry, inert atmosphere, the oxide layer is quickly removed, and the friction remains low. However, the presence of surface oxides prolongs the break-in period, reducing the friction life.

One of the most critical factors affecting the lubrication performance of MoS<sub>2</sub> films is the humid environment. For many years, the reaction between water molecules and the active sites or unsaturated bonds at the edge of the MoS<sub>2</sub> basal plane (Fig. 10) to form MoO<sub>3</sub> has been recognized as the mechanism responsible for the increased friction and wear of MoS<sub>2</sub> in humid environments. There are two possible chemical reactions involved [59, 72–75]:





**Fig. 10** Schematic representation of the reaction mechanism of MoS<sub>2</sub> films with water [18]. (c) reproduced from ref. 3. Copyright ©2012 J Mater Sci



In addition to converting MoS<sub>2</sub> to non-lubricating MoO<sub>3</sub>, H<sub>2</sub>S gas is produced in reaction (i), and although H<sub>2</sub>S does not directly affect the tribological properties, it causes loss of S element. In reaction (ii), acidic H<sub>2</sub>SO<sub>4</sub> is produced, which can cause corrosion of the metal substrate. The combination of these factors significantly reduces the lubrication performance and wear life of MoS<sub>2</sub> in humid environments.

However, some recent experimental studies [57, 65, 67, 76, 77] and simulations [76, 78] have shown that water does not promote MoS<sub>2</sub> oxidation at room temperature. In a humid N<sub>2</sub> environment, no O signal was detected on the wear surface of the film, suggesting that water did not cause film oxidation [57]. This result is consistent with the Raman spectroscopy analysis by Windom et al. Humid environments have little effect on oxidation compared to dry air or O<sub>2</sub> environments [67]. In addition, an appropriate increase in temperature in humid air improves the tribological properties of the films, which suggests that water adsorption/desorption is a reversible process, i.e., water is physically adsorbed rather than chemically adsorbed [57, 77].

Water adsorption and desorption calculations on MoS<sub>2</sub> films have shown [76, 78, 79] that oxidation at the edge locations is much less likely than water molecule adsorption. Water molecules can dissociate into O and OH and adsorb at all edge sites and defects in MoS<sub>2</sub> films. Levita [78] used molecular dynamics calculations to simulate the interaction between water and MoS<sub>2</sub> bilayers, where the insertion of water molecules into the interlayers significantly inhibited interlayer sliding. For a given condition, the number of water molecules at the interface increased, and the sliding distance and velocity

decreased, consistent with viscous friction. It has also been suggested that water vapor adsorbed at MoS<sub>2</sub> film defects forms liquid water due to capillary condensation, which inhibits the easy shear effect between the substrate layers and increases friction [58].

Curry [80] found that the friction coefficients of MoS<sub>2</sub> films with a high degree of orientation remained almost unchanged in dry and humid environments. In contrast, the tribological behavior of amorphous MoS<sub>2</sub> films was very dependent on the environment. Therefore, the authors concluded that water in humid environments does not affect the shear behavior of MoS<sub>2</sub> films that already have a highly ordered structure but rather restricts the formation of induced ordered laminar structures in amorphous MoS<sub>2</sub> films during friction. It also suggests that highly ordered structures can significantly improve the tribological properties of MoS<sub>2</sub> films in humid environments. Chhowalla [16] prepared films consisting of fullerene MoS<sub>2</sub> nanoparticles by localized high-voltage arc discharge method and observed ultra-low friction and wear in humid environments, which was mainly attributed to the presence of curved S-Mo-S hexagonal planes, which reduces the number of dangling bonds exposed at the edges of the planes, prevents the oxidation of Mo atoms and maintains the lamellar structure.

In summary, the primary mechanisms for the deterioration of the lubrication properties of MoS<sub>2</sub> films in humid environments include two aspects: first, physical effects, where water molecules are physically adsorbed on the surface of the film, and hydrogen bonding exists between the basal planes [76, 81], which destroys the easily shearable lamellar structure [57, 82], increases adhesion [58], and restricts the friction film growth and reorientation [80], resulting in the degradation of the tribological properties; and second, chemical effects. Water molecules react with the active sites or unsaturated

bonds at the edge of the MoS<sub>2</sub> substrate to form MoO<sub>3</sub> oxides, H<sub>2</sub>S, and H<sub>2</sub>SO<sub>4</sub>, which reduce the tribological properties.

#### 4.2 Effects of temperature

The maximum temperature at which MoS<sub>2</sub> films provide adequate lubrication is highly dependent on the operating environment (e.g., vacuum, inert atmosphere, and humidity) and the microstructure of the film (e.g., crystal structure, doping, density, and surface roughness).

In atmospheric environments, high temperatures promote the oxidation of active sites, grain boundaries, and defects at MoS<sub>2</sub> edges by O<sub>2</sub> and water to produce MoO<sub>2</sub> and MoO<sub>3</sub>, and the oxides destroy the characteristics prone to shear rearrangement at MoS<sub>2</sub> friction interfaces to produce high friction and wear. The oxidation mechanism is that O<sub>2</sub> and water are first physically adsorbed on the MoS<sub>2</sub> surface. When the temperature increases, a chemical reaction forms molybdenum oxide. Therefore, there exists a transition temperature [77], below which an increase in temperature causes the resolution of physically adsorbed O<sub>2</sub> and water and a decrease in the coefficient of friction and wear rate; when the temperature exceeds the transition temperature, the rate of oxidation increases significantly, increasing the coefficient of friction and wear. Studies have shown that the transition temperature is between 100 and 300°C [49, 67, 83, 84]. Kubart [83] and Arslan [84] found that pure MoS<sub>2</sub> and MoS<sub>2</sub>/Nb composite films have the lowest friction coefficients and wear rates at 100°C, respectively. The coefficient of friction increases gradually when the temperature exceeds 100°C, and the wear rate increases sharply after 300°C. The upper-temperature limit for long-term lubrication of MoS<sub>2</sub> films in atmospheric or oxygen environments is 300~350°C, and for short-term lubrication, the temperature can be 400~500°C.

The thermal stabilization temperature of MoS<sub>2</sub> is dramatically increased in a high vacuum environment and inert atmosphere. NASA study reported [85] that the decomposition and weight loss of MoS<sub>2</sub> in ultrahigh vacuum (10<sup>-9</sup>Torr) starts at 930°C. However, when friction was performed in a high vacuum from 10<sup>-6</sup> to 10<sup>-8</sup>Torr, the friction coefficient remained unchanged below 500°C and significantly increased above 600°C. The thermal decomposition rate of MoS<sub>2</sub> increases rapidly at temperatures higher than 500°C in vacuum > 10<sup>-5</sup>Pa. The limiting temperature for effective lubrication is 400~500°C, which may be due to the presence of a certain amount of O<sub>2</sub> and water vapor still in the vacuum and the oxidation of the film at high temperatures [49, 86].

The lubrication behavior of MoS<sub>2</sub> films is limited by the high temperature, and the high-temperature lubrication performance of MoS<sub>2</sub>-based films can be

effectively enhanced by preparing films with (002) crystalline facets optimally oriented and by adding metal elements or oxides to prepare nanocomposite films. Wang Jihui found that when the working air pressure was between 0.15Pa and 0.4Pa, the prepared MoS<sub>2</sub> films were base plane oriented with (002) planes parallel to the substrate, and the inert base planes were exposed to air and the films were denser and less susceptible to oxidation [87]. It is in agreement with Curry, who found that highly ordered MoS<sub>2</sub> films with basal plane orientation exhibit higher oxidation resistance [68]. A.T.Alpas [88, 89] significantly improved the high-temperature lubrication properties of MoS<sub>2</sub>/Ti composite films prepared by Ti doping. The composite films exhibited low friction and low wear in the room temperature range of ~350°C; the friction and wear rate coefficient increased dramatically when the temperature exceeded 400°C. Paul [90] compared the high-temperature wear properties of pure MoS<sub>2</sub>, Ti-MoS<sub>2</sub>, and Sb<sub>2</sub>O<sub>3</sub>/Au-MoS<sub>2</sub> films, and the results pointed out that the pure MoS<sub>2</sub> had the lowest wear at 30°C, the highest wear at 100°C; Sb<sub>2</sub>O<sub>3</sub>/Au-MoS<sub>2</sub> film produces grain-abrasion at 30°C and has the best performance at 100°C; Ti-MoS<sub>2</sub> film, on the other hand, has better tribological properties at both 30°C and 100°C.

Low temperature also has an essential effect on the tribological properties of MoS<sub>2</sub> films, and the mechanism is different from high-temperature oxidative decomposition. In 1976, Karapetyan [91] first found that the coefficient of friction of MoS<sub>2</sub> increased by a factor of two when the temperature was reduced from 250 to 200K. The friction coefficient of MoS<sub>2</sub> was found to increase by a factor of two when the temperature was lowered from 250 to 200K. The friction coefficient of MoS<sub>2</sub> was found to increase by a factor of two when the temperature was decreased from 250 to 200K. Initially, it was thought that it might be caused by the test conditions (non-vacuum). However, recently, Lince [92] measured the tribological properties of sodium silicate-bound MoS<sub>2</sub> coatings and sputter-deposited Au-MoS<sub>2</sub> films (nano-complexes of amorphous MoS<sub>2</sub> and nanoparticles of Au) at temperatures ranging from 100 to 300K in a high-vacuum condition (~1×10<sup>-8</sup>Torr). At temperatures ranging from 220K and above, both materials have low friction coefficients. However, the friction coefficients of both materials increase about two times when the temperature drops below 220K. Zhao [93] measured the friction on the surface of single-crystalline MoS<sub>2</sub> using ultrahigh-vacuum AFM, and the friction coefficients were elevated by at least 30 times when the temperature was decreased from 250 to 200K. Comparing the above results that the friction coefficient is expected to increase by at least a factor of two when MoS<sub>2</sub> films are used in ultra-low

temperature mechanisms in space which concluded by the scholars.

Curry [94] correlated the macroscopic interfacial shear strength of MoS<sub>2</sub> with temperature, considered the sliding energy barrier, and developed a predictive model to predict the relationship between interfacial interlayer shear strength and temperature. Molecular dynamics calculations simulated the variation of MoS<sub>2</sub> interlayer shear strength with temperature, and the results showed that the interlayer shear strength increased from 20 to 55 MPa as the temperature decreased from 300 to 30 K, corresponding to the friction coefficient increasing from 0.08 to 0.16. The MoS<sub>2</sub> friction temperature dependence is related to the thermal activation behavior, which is exhibited at 220~500 K with an activation barrier of about 0.3 eV. The friction behavior is nonthermally activated below 220 K. However, the thermally activated friction behavior is limited to negligible friction. However, the thermally activated friction behavior is limited to the case of negligible wear. In contrast, the transition from thermally activated friction to nonthermally activated friction directly results from wear [92]. However, the results of studies on the low-temperature tribological behavior of MoS<sub>2</sub> (from the cryogenic state to around 150 °C) are still highly divergent, with some studies suggesting that the friction coefficient increases monotonically with decreasing temperature [52, 94–96], whereas some studies [48, 91–93, 97] have shown the existence of a critically low temperature, above which the friction coefficient increases significantly with decreasing temperature. However, the friction coefficient remains constant at the critical low temperature the friction coefficient remains constant.

### 4.3 Effects of doping

Dopants have been used for decades to improve the tribological properties of MoS<sub>2</sub> films. There are many types of dopants, including non-metallic (C, O, N, P, B et al.) [41, 44, 53, 98–100], metallic (Ti, Cr, Ni, Zr, Nb, Pb, Au et al.) [14, 47, 48, 50, 84, 90, 101–104], oxides (Sb<sub>2</sub>O<sub>3</sub>, PbO) [42, 48, 105], and rare-earth fluorides (LaF<sub>3</sub> et al.) [106, 107]. Dopants can be dispersed in MoS<sub>2</sub> films by replacing lattice atoms and inserting into gaps between lattice atoms, interlayers, or independent phases.

It has long been found that adding graphite to rubbed or bonded MoS<sub>2</sub> coatings significantly reduces the coefficient of friction of such coatings in air and improves wear life [41, 108]. When rubbing in air, oxidation occurs within the MoS<sub>2</sub> layer, forming molybdenum oxide and SO<sub>2</sub> gas, molar volume contraction, oxidative corrosion resulting in layers that are not easily sheared, gas adsorption and volume contraction leading to the generation of bubbles, and large amounts of gas bubbles peeling off the

delamination is the root cause of the catastrophic failure of the MoS<sub>2</sub> film. Synergistic lubrication effects of MoS<sub>2</sub> and graphite in the air include: (1) Graphite laminates in the air have better lubrication performance, which compensates for the failure of MoS<sub>2</sub> laminates and prolongs the interlayer shear at the sliding interface; (2) The graphite crystals oxidize very slowly, which to a certain extent acts as an antioxidant and moisture/O<sub>2</sub> scavenger; (3) The dense graphite structure acts as a diffusion barrier for moisture and O<sub>2</sub>, reducing friction and improving the lifetime. Recent studies have shown [2, 56] that heterojunctions formed by graphene and MoS<sub>2</sub> alkene form incommensurate heterogeneous contacts at the friction interface and reduce frictional wear, which explains the synergistic lubrication mechanism of MoS<sub>2</sub> and graphite from a microscopic point of view.

Ti and Au are the most widely studied and applied metal dopants. According to the film TEM analysis, after Ti doping, its atoms are uniformly distributed in MoS<sub>2</sub>, there are no Ti nanoclusters or delamination, and the films show a homogeneous structure [86, 109–111] (e.g., Fig. 11 (a)). Ti atoms are either inserted between the MoS<sub>2</sub> layers [101] or replaced with Mo [112], all present in the solid solution form. The Ti-doped films have a columnar structure, and as the Ti content increases, the film density increases, the hardness rises, the oxidation resistance improves, and the tribological properties of the films at high temperatures and in humid air are significantly improved [88, 89, 101]. However, there exists a Ti content limit of about 16~18 at.% above which the performance decreases [101].

Au is dispersed in the MoS<sub>2</sub> substrate as Au nanoparticles (or nanoclusters) after doping into the MoS<sub>2</sub> film (e.g., Fig. 11 (b)), and the size of the nanoparticles is dependent on the deposition temperature [110, 113, 115]. The hardness of the film is reduced by Au doping, and thus, the mechanism of improvement of the tribological properties is different from that of Ti. Scharf et al. suggested that the frictional process involves the Au nanoparticles at the aggregation of Au nanoparticles at the subsurface of the friction interface, providing loading support to support the sliding of the surface MoS<sub>2</sub> substrate layer by layer [49, 113] Fig. 11(c,d,e). The optimal amount of Au depends on the contact stress, with a low Au content being better at high stresses to form a sufficient friction film of MoS<sub>2</sub> at the friction interface and a high Au content being good at low stresses for a thin and homogeneous MoS<sub>2</sub> film to be transferred [115, 116].

Sb<sub>2</sub>O<sub>3</sub> is one of the most commonly used additives in MoS<sub>2</sub> lubricants. Doping Sb<sub>2</sub>O<sub>3</sub> produces grain refinement, MoS<sub>2</sub> microcrystals dispersed in amorphous Sb<sub>2</sub>O<sub>3</sub>, and composite films with higher density and hardness. Sb<sub>2</sub>O<sub>3</sub> has been reported to act as a diffusion



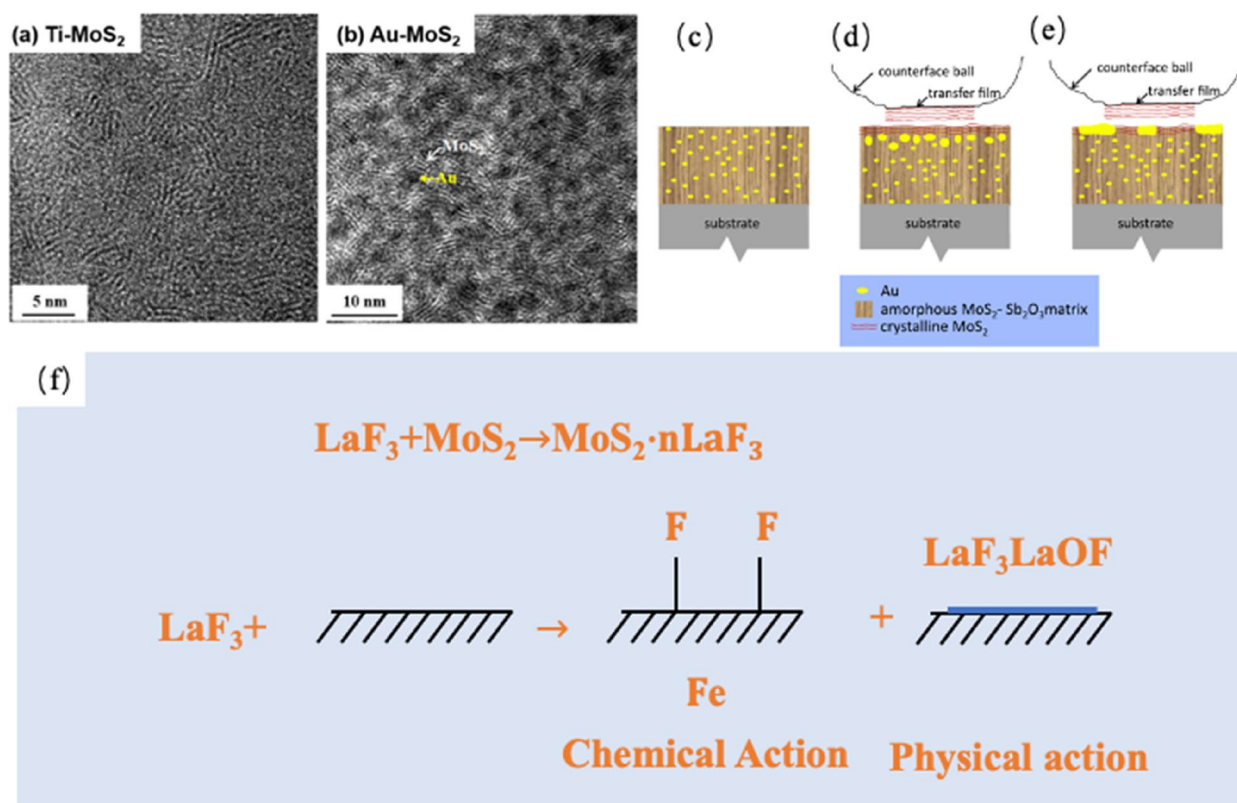


**Fig. 11** (a) HRTEM photographs of Ti-MoS<sub>2</sub> films [86] (b) HRTEM photographs of Au-MoS<sub>2</sub> films [113] Schematic diagram of the lubrication mechanism of MoS<sub>2</sub>/Sb<sub>2</sub>O<sub>3</sub>/Au composite films in different environments (c) Unworn surfaces in dry nitrogen (d) Worn surfaces in dry nitrogen and (e) Worn surfaces in air at RH50% [49] (f) Mechanisms of fluoride's action to improve the lubrication film of MoS<sub>2</sub> [114]. (a) reproduced from ref. 71. Copyright © 2022 Tribology; (a) reproduced from ref. 99. Copyright © 2013 ACS Appl Mater Interfaces; (c~e) reproduced from ref. 31. Copyright © 2010 Published by Elsevier Ltd. on behalf of Acta Materialia Inc; (f) reproduced from ref. 100 Copyright © Taylor & Francis Group, LLC

barrier and antioxidant, preventing heat and O diffusion and reducing MoS<sub>2</sub> oxidation, therefore improving the tribological properties of the films at high temperatures and in humid air [42, 48, 72]. Rare earth fluorides (LaF<sub>3</sub>) have also been used to improve the oxidation resistance, humidity resistance, corrosion resistance, and tribological properties of MoS<sub>2</sub> films [106, 107]. The addition of LaF<sub>3</sub> saturates the active prisms of MoS<sub>2</sub> by competitive adsorption with them, reducing their activity to interact with water and O<sub>2</sub> in the air and improving the oxidation and humidity resistance of MoS<sub>2</sub>. LaF<sub>3</sub> can also interact with the metal surface in chemical and physical interaction, passivating it and improving its corrosion resistance [114] (Fig. 11 (f)). In addition, LaF<sub>3</sub> forms a interfacial strong bond with the MoS<sub>2</sub> substrate and improves the friction interface densities, thus improving the wear resistance of MoS<sub>2</sub> films [117, 118].

Multi-component co-doped MoS<sub>2</sub> films can exploit the synergistic mechanism between different dopants to achieve better tribological properties. Au/Sb<sub>2</sub>O<sub>3</sub>. Co-doped MoS<sub>2</sub> composite films have been widely studied,

and composite films consisting of 82%MoS<sub>2</sub>, 11%Sb<sub>2</sub>O<sub>3</sub>, and 7%Au (molar ratio) have even better tribological properties. The wear rate of the Au/Sb<sub>2</sub>O<sub>3</sub> doped MoS<sub>2</sub> films is lower than that of the single Sb<sub>2</sub>O<sub>3</sub> doped MoS<sub>2</sub> films at room temperature [47]. Sb<sub>2</sub>O<sub>3</sub> doped MoS<sub>2</sub> films have a wear rate that is an order of magnitude lower than single Sb<sub>2</sub>O<sub>3</sub> doping [48], as well as low friction and long-life performance in moist air and dry N<sub>2</sub> [49]. A schematic of the lubrication mechanism of Sb<sub>2</sub>O<sub>3</sub>/Au/MoS<sub>2</sub> composite films in different environments is given in Fig. 10 (c),(d), and (e). In dry N<sub>2</sub>, the furthest surface of the abrasion marks consists of crystalline MoS<sub>2</sub> with (002) orientation, completely covering the Au nanoclusters. In contrast, the dyadic surface transfer film is a MoS<sub>2</sub> substrate with the same (002) orientation. The abrasion mark interface in the air is a complex of Au nanoclusters and crystalline MoS<sub>2</sub>. Other co-doped films such as YSZ/Au/DLC/MoS<sub>2</sub> [119], Pb/Ti/MoS<sub>2</sub> [120], Sb<sub>2</sub>O<sub>3</sub>/C/MoS<sub>2</sub> [43, 48] achieved multi-environmental adaptability of tribological properties, and Mo<sub>2</sub>N/Ag/MoS<sub>2</sub> [121], Ti/TiB<sub>2</sub>/MoS<sub>2</sub> [109] realized a room temperature to 500°C range

of self-lubricating properties over a wide temperature domain.

Doped MoS<sub>2</sub> films continue to receive attention from researchers, and probing the mechanisms by which dopants improve the oxidation resistance and tribological properties of MoS<sub>2</sub> films remains an active research topic. Regarding antioxidant properties, doping affects MoS<sub>2</sub> crystal growth, reduces grain size, and transforms MoS<sub>2</sub> into an amorphous structure, increasing film densification. Amorphous and higher densities can reduce grain boundaries, defects, edge active sites, etc., to improve oxidation resistance. Finally, some dopants, such as Ti, preferentially combine with oxygen to form oxides and protect MoS<sub>2</sub>. In terms of tribological properties, different mechanisms have been proposed by different scholars to explain the effect of dopants on friction wear life, with the most widely cited mechanisms being amorphization, density increase, and hardness enhancement. Due to the MoS<sub>2</sub> crystal structure distortion caused by doping, the film is transformed from a crystalline to an amorphous structure, with an increase in density and elevated hardness, contributing to the improvement of friction wear. For multi-doped MoS<sub>2</sub> films, the synergistic effect between different dopants, utilizing the lubrication properties of different lubricants in different environments, is the mechanism for the environmental adaptation of tribological properties.

#### 4.4 Future development and outlook for MoS<sub>2</sub> films

1. Development of TMDs Smart Adaptive Lubrication Films. The application areas are getting more comprehensive based on the excellent lubrication properties of TMDs films. Even in spacecraft applications, spacecraft are usually stored in air and coastal environments for extended periods before launch. As application needs continue to evolve, TMDs films must adapt to complex environments, higher temperatures, harsh operating conditions, variable shapes, multifunctional requirements, and more. Therefore, developing environment-adaptive, temperature-adaptive, working condition-adaptive, shape-adaptive, and multifunctional-adaptive smart lubrication films for TMDs is a cutting-edge topic and research hotspot in tribology. Although a lot of research work has been carried out and significant progress has been made, it involves numerous scientific and technological issues that need to be overcome by a large amount of research.

2. Active design of dopant and structurally controllable preparation of TMDs. Doped MoS<sub>2</sub> films have made significant progress and have been widely used in the past decades, but there are also new challenges

and opportunities. First, many dopant elements have been studied at home and abroad. However, due to different preparation techniques, deposition conditions, tribological experiments, and confidentiality reasons, the comparability between data could be better, and some research results are contradictory. Secondly, most of the studies are still experiment-oriented and have not yet considered the atomic nuclear electronic structure of the dopant, as well as the micro-interaction mechanism with the molecular structure of the TMDs, and the position of the dopant in the TMDs, the structural distortions induced, and how it affects the growth process are still not clear. Third, not all elements can be used for doping, and doping elements with competitive bonding coordination will destroy the lamellar structure of TMDs and deteriorate the lubrication performance. Therefore, when faced with specific application requirements in the future, there is no way to actively select suitable dopants and actively control the microstructure of TMDs, which is still based on experience and experimentation.

3. Analytical equipment for in situ performance evaluation. Despite the agreement on trends in the effects of humidity, temperature, and vacuum on the tribological behavior of TMDs (especially MoS<sub>2</sub>), significant differences in mechanisms remain, mainly due to the difficulty in carrying out the effects of single factors (e.g., water, oxygen, as well as others), as well as the lack of in situ analytical techniques. Therefore, designing and constructing new test rigs that can individually control the various influencing factors and provide in-situ high-resolution analysis of sliding interfaces could make great strides in understanding the solid lubrication mechanisms of TMDs.

4. Long-life reliability testing techniques. For new TMDs lubrication films, many tests must be conducted to obtain sufficient data before actual application. However, many applications usually operate in extreme environments with long lifetimes, such as 10~20year space missions in ultra-high vacuum and extreme temperatures. These conditions are difficult to reproduce in a laboratory environment. In addition, while space applications face vacuum levels that can reach below 10<sup>-10</sup>Pa, vacuum friction equipment in the laboratory hardly reaches 10<sup>-8</sup>Pa. The low vacuum level means small amounts of water, oxygen, and hydrocarbon gases are unavoidable. It has been shown that even minimal amounts of water, oxygen, and other contaminants can significantly affect the lubrication performance and life of TMDs. Therefore, there are still significant limitations and challenges in areas such as test rigs and technologies related

to simulating ultra-high vacuum and extremely low temperatures for up to ten years.

**5. Computational Simulation Techniques.** Given the limitations of experimental testing, computational simulation techniques have been emphasized. By describing the interactions between atoms through computational simulation and capturing the formation and breakage of bonds during friction, it is possible to gain insight into the structural and chemical changes occurring at the sliding interface from the atomic molecular-electronic level, thus probing the nature of lubrication and wear. Meanwhile, the interaction between dopant atoms and TMDs molecules is computationally modeled to predict the effect of dopants on the structure and tribological properties of TMDs and to propose doping strategies. Computational simulation is an ideal exploratory tool in proactively tuning and selecting dopants to optimize the tribological performance for specific application scenarios, and its development becomes an important direction for future research.

#### Acknowledgements

Strategic Priority Research Program of the Chinese Academy of Sciences (Grant No. XDB 0470202), Youth Innovation Promotion Association of Chinese Academy of Sciences (Grant No. Y202084), Key Program of the Lanzhou Institute of Chemical Physics, CAS (Grant No. KJZLZD-3 and ZYFZFX-4), Key Science and Technology Program of Gansu Province (Grant No. 22ZD6GA002), National Natural Science Foundation of China (Grant No. 52275222).

#### Authors' contributions

Hongxuan Li: Conceptualization, Project administration, Methodology, Writing-Review & Editing, Supervision, Funding acquisition. Shifan Ju: Conceptualization, Methodology, Formal analysis, Investigation, Writing-Original. Li Ji: Conceptualization, Supervision, Funding acquisition. Xiaohong Liu: Writing-Review & Editing. Jianmin Chen: Project administration, Resources. Huidi Zhou: Project administration, Resources. Xiaoqin Zhao: Writing-Review & Editing, Supervision, Project administration.

#### Availability of data and materials

"Data availability is not applicable to this article as no new data were created or analyzed in this study."The data in the article are in the references.

#### Declarations

##### Competing interests

Hongxuan Li is a member of the editorial board of this journal. He was not involved in the editorial review or the decision to publish this article. All authors declare that there are no competing interests.

Received: 17 October 2023 Revised: 2 December 2023 Accepted: 4 December 2023  
Published online: 19 December 2023

#### References

- Martin JM, Donnet C, Le MT et al (1993) Superlubricity of molybdenum disulphide. *Phys Rev B* 48(14):10583–10586. <https://doi.org/10.1103/PhysRevB.48.10583>
- Li P, Ju P, Ji L et al (2020) Toward robust macroscale superlubricity on engineering steel substrate. *Adv Mater* 32(36):2002039. <https://doi.org/10.1002/adma.202002039>
- Song H, Ji L, Li HX, Wang JQ, Liu XH, Zhou HD, Chen JM (2017) Self-forming oriented layer slip and macroscale super-low friction of graphene. *Appl Phys Lett* 110:073101. <https://doi.org/10.1063/1.4975979>
- Luo JB, Zhou X (2020) Superlubricative engineering—Future industry nearly getting rid of wear and frictional energy consumption. *Friction* 8(4):643–665. <https://doi.org/10.1007/s40544-020-0393-0>
- Leven I, Krepel D, Shemesh O, Hod O. Robust superlubricity in graphene/h-BN heterojunctions. *J Phys Chem Lett*. <https://doi.org/10.1021/jz301758c>.
- Berman D, Erdemir A, Sumant AV (2014) Graphene: a new emerging lubricant. *Mater Today* 17:31–42. <https://doi.org/10.1016/j.mattod.2013.12.003>
- Wang LF, Ma TB, Hu YZ, Zheng Q, Wang H, Luo J (2014) Superlubricity of two-dimensional fluorographene/MoS<sub>2</sub> heterostructure: a first-principles study. *Nanotechnology* 25:385701. <https://doi.org/10.1088/0957-4484/25/38/385701>
- Berman D, Erdemir A, Sumant AV (2018) Approaches for achieving superlubricity in two-dimensional materials. *ACS Nano* 12:2122–2137. <https://doi.org/10.1021/acsnano.7b09046>
- Enke K, Dimigen H, Hübsch H (1980) Frictional properties of diamondlike carbon layers. *Appl Phys Lett*. 36:291–292. <https://doi.org/10.1021/10.1063/1.91465>
- Donnet C (1996) Advanced solid lubricant coatings for high vacuum environments. *Surf Coat Technol* 80:151–156
- Erdemir A, Eryilmaz OL, Fenske G (2000) Synthesis of diamondlike carbon films with superlow friction and wear properties. *J Vac Sci Technol A* 18:1987–1992. <https://doi.org/10.1116/1.582459>
- Dickinson RG, Pauling L et al (2001) The crystal structure of molybdenite. *Acta Crystallogr A* 45(4):207–210. <https://doi.org/10.1021/ja01659a020>
- Ding XZ, Zeng XT, He XY et al (2010) Tribological properties of Cr- and Ti-doped MoS<sub>2</sub> composite coatings under different humidity atmosphere. *Surf Coat Technol* 205(1):224–231. <https://doi.org/10.1016/j.surfcoat.2010.06.041>
- Yin X, Jin J, Chen X et al (2021) A new pathway for superlubricity in a multilayered MoS<sub>2</sub>-Ag film under cryogenic environment. *Nano Lett* 21(24):10165–10171. <https://doi.org/10.1021/acs.nanolett.1c02605>
- Martion JM (2007) 13-Superlubricity of Molybdenum Disulfide [M]. In: Superlubricity. Erdemir A, Martin J-M eds. Amsterdam: Elsevier Science BV 207–25. <https://doi.org/10.1016/B978-044452772-1/50044-5>.
- Chhowalla M, Amaratunga GAJ (2000) Thin films of fullerene-like MoS<sub>2</sub> nanoparticles with ultra-low friction and wear. *Nature* 407(6801):164–167. <https://doi.org/10.1038/35025020>
- Radisavljevic B, Radenovic A, Brivio J et al (2011) Single-layer MoS<sub>2</sub> transistors. *Nature Nanotech* 6:147–150. <https://doi.org/10.1038/nnano.2010.279>
- Scharf TW, Prasad SV (2013) Solid lubricants: a review. *J Mater Sci* 48(2):511–531. <https://doi.org/10.1007/s10853-012-7038-2>
- Liu WM, Weng LJ, Sun JY (2009) Handbook of space lubrication materials and technologies [M]. Handbook of space lubrication materials and technologies.
- Spalvins T (1969) Deposition of MoS<sub>2</sub> films by physical sputtering and their lubrication properties in vacuum. *A S L E Transactions* 12(1):36–43. <https://doi.org/10.1080/05698196908972244>
- Yang JF, Parakash B, Hardell J et al (2012) Tribological properties of transition metal di-chalcogenide based lubricant coatings. *Front Mater Sci* 6(2):116–127. <https://doi.org/10.1007/s11706-012-0155-7>
- Buck V (1991) Lattice parameters of sputtered MoS<sub>2</sub> films. *Thin Solid Films* 198(1):157–167. [https://doi.org/10.1016/0040-6090\(91\)90334-T](https://doi.org/10.1016/0040-6090(91)90334-T)
- Bertrand PA (1989) Orientation of rf-sputter-deposited MoS<sub>2</sub> films. *J Mater Res* 4(1):180–184
- Hilton MR, Bauer R, Didziulis SV et al (1992) Structural and tribological studies of MoS<sub>2</sub> solid lubricant films having tailored metal-multilayer nanostructures. *Surf Coat Technol* 53(1):13–23. [https://doi.org/10.1016/0257-8972\(92\)90099-V](https://doi.org/10.1016/0257-8972(92)90099-V)
- Vazirisereshk MR, Martini A, Strubbe DA et al (2019) Solid lubrication with MoS<sub>2</sub>: a review. *Lubricants* 7(7):57. <https://doi.org/10.3390/lubricants7070057>



26. Roberts EW (2012) Space tribology: its role in spacecraft mechanisms. *J Phys D Appl Phys* 45(50):503001. <https://doi.org/10.1088/0022-3727/45/50/503001>
27. Lince JR, Loewenthal SH, Clark CS (2016) Degradation of sputter-deposited nanocomposite MoS<sub>2</sub> coatings for NIRCams during storage in air, F.
28. Krantz T, Hakun C, Cameron Z, et al (2018) Performance of MoS<sub>2</sub> coated gears exposed to humid air during storage, F [C].
29. Krause O, Muller F, Birkmann, et al (2010) High-precision cryogenic wheel mechanisms of the JWST/MIRI instrument: Performance of the flight models. *Proc. SPIE* 7739:773918. <https://doi.org/10.1117/12.856887>.
30. Donnet C, Le Mogne T, Martin JM (1993) Superlow friction of oxygen-free MoS<sub>2</sub> coatings in ultrahigh vacuum. *Surface Coat Technol* 62(1):406–11. [https://doi.org/10.1016/0257-8972\(93\)90275-5](https://doi.org/10.1016/0257-8972(93)90275-5)
31. Martin JM, Pascal H, Donnet C et al (1994) Superlubricity of MoS<sub>2</sub>: crystal orientation mechanisms. *Surf Coat Technol* 68–69:427–432. [https://doi.org/10.1016/0257-8972\(94\)90197-X](https://doi.org/10.1016/0257-8972(94)90197-X)
32. Hirano S (1990) Atomistic locking and friction. *Phys Rev B: Condens Matter* 41(17):11837–11851. <https://doi.org/10.1103/PhysRevB.41.11837>
33. Shinjo K, Hirano M (1993) Dynamics of friction: superlubric state. *Surf Sci* 283(1):473–478. [https://doi.org/10.1016/0039-6028\(93\)91022-H](https://doi.org/10.1016/0039-6028(93)91022-H)
34. Hirano M, Shinjo K (1993) Superlubricity and frictional anisotropy. *Wear* 168(1):121–125. [https://doi.org/10.1016/0043-1648\(93\)90207-3](https://doi.org/10.1016/0043-1648(93)90207-3)
35. Donnet C, Martin JM, Le MT, et al (1994) The origin of super-low friction coefficient of MoS<sub>2</sub> coatings in various environments. Dowson D, Taylor CM, Childs THC, et al. *Tribology Series*. Elsevier. 277–84. [https://doi.org/10.1016/S0167-8922\(08\)70317-1](https://doi.org/10.1016/S0167-8922(08)70317-1).
36. Lince JR, Hilton MR, Bommannavar AS (1995) EXAFS of sputter-deposited MoS<sub>2</sub> films. *Thin Solid Films* 264(1):120–134
37. Sokoloff JB (1990) Theory of energy dissipation in sliding crystal surfaces. *Phys Rev B* 42(1):760–765. <https://doi.org/10.1103/physrevb.42.760>
38. Hou K, Han M, Liu X et al (2018) In situ formation of spherical MoS<sub>2</sub> nanoparticles for ultra-low friction. *Nanoscale* 10(42):19979–19986. <https://doi.org/10.1039/C8NR06503A>
39. Donnet C, Martin JM, Le MT et al (1996) Super-low friction of MoS<sub>2</sub> coatings in various environments. *Tribol Int* 29(2):123–128. [https://doi.org/10.1016/0301-679X\(95\)00094-K](https://doi.org/10.1016/0301-679X(95)00094-K)
40. Voevodin AA, Fitz TA, Hu JJ et al (2002) Nanocomposite tribological coatings with “chameleon” surface adaptation. *J Vac Sci Technol, A* 20(4):1434–1444. [https://doi.org/10.1007/1-4020-2222-0\\_1](https://doi.org/10.1007/1-4020-2222-0_1)
41. Gardos MN (1988) The synergistic effects of graphite on the friction and Wear of MoS<sub>2</sub> films in air. *Tribol Trans* 31(2):214–227. <https://doi.org/10.1080/10402008808981817>
42. Zabinski JS, Donley MS, Mcdevitt NT (1993) Mechanistic study of the synergism between Sb<sub>2</sub>O<sub>3</sub> and MoS<sub>2</sub> lubricant systems using Raman spectroscopy. *Wear* 165(1):103–108. [https://doi.org/10.1016/0043-1648\(93\)90378-Y](https://doi.org/10.1016/0043-1648(93)90378-Y)
43. Zabinski JS, Bultman JE, Sanders JH et al (2006) Multi-environmental lubrication performance and lubrication mechanism of MoS<sub>2</sub>/Sb<sub>2</sub>O<sub>3</sub>/C composite films. *Tribol Lett* 23(2):155–163. <https://doi.org/10.1007/s11249-006-9057-0>
44. Wu Y, Li H, Ji L et al (2013) Structure, mechanical, and tribological properties of MoS<sub>2</sub>/a-C: H composite films. *Tribol Lett* 52(3):371–380. <https://doi.org/10.1007/s11249-013-0216-9>
45. Li XY, Ji L, Liu XH, Sun CF, Li HX. Vacuum supergliding behavior of MoS<sub>2</sub>-C heterogeneous composite films and its mechanism. *Tribology*. <https://doi.org/10.16078/j.tribology.2022174>.
46. Hilton MR, Fleischauer PD (1992) Applications of solid lubricant films in spacecraft. *Surf Coat Technol* 54–55:435–441
47. Zabinski JS, Donley MS, Walck SD et al (1995) The effects of dopants on the chemistry and tribology of sputter-deposited MoS<sub>2</sub> films. *Tribol Trans* 38(4):894–904. <https://doi.org/10.1080/10402009508983486>
48. Hamilton MA, Alvarez LA, Mauntler NA et al (2008) A possible link between macroscopic Wear and temperature dependent friction behaviors of MoS<sub>2</sub> coatings. *Tribol Lett* 32(2):91–98. <https://doi.org/10.1007/s11249-008-9366-6>
49. Scharf TW, Kotula PG, Prasad SV (2010) Friction and wear mechanisms in MoS<sub>2</sub>/Sb<sub>2</sub>O<sub>3</sub>/Au nanocomposite coatings. *Acta Mater* 58(12):4100–4109. <https://doi.org/10.1016/j.actamat.2010.03.040>
50. Singh H, Mutyala KC, Evans RD et al (2015) An investigation of material and tribological properties of Sb<sub>2</sub>O<sub>3</sub>/Au-doped MoS<sub>2</sub> solid lubricant films under sliding and rolling contact in different environments. *Surf Coat Technol* 284:281–289. <https://doi.org/10.1016/j.surfcoat.2015.05.049>
51. Kwanghua CR (2020) Temperature-dependent negative friction coefficients in superlubric molybdenum disulfide thin films. *J Phys Chem Solids* 143:109526. <https://doi.org/10.1016/j.jpcs.2020.109526>
52. Curry JF, Babuska TF, Brumbach MT et al (2016) Temperature-dependent friction and Wear of MoS<sub>2</sub>/Sb<sub>2</sub>O<sub>3</sub>/Au nanocomposites. *Tribol Lett* 64(1):18. <https://doi.org/10.1007/s11249-016-0748-x>
53. Lince JR, Hilton MR, Bommannavar AS (1990) Oxygen substitution in sputter-deposited MoS<sub>2</sub> films studied by extended X-ray absorption fine structure, X-ray photoelectron spectroscopy and X-ray diffraction. *Surf Coat Technol* 43–44:640–651. [https://doi.org/10.1016/0257-8972\(90\)90008-Z](https://doi.org/10.1016/0257-8972(90)90008-Z)
54. Yu G, Qian Q, Li D et al (2021) The pivotal role of oxygen in establishing superlow friction by inducing the in situ formation of a robust MoS<sub>2</sub> transfer film. *J Colloid Interface Sci* 594:824–835. <https://doi.org/10.1016/j.jcis.2021.03.037>
55. Wang L, Zhou X, Ma T et al (2017) Superlubricity of a graphene/MoS<sub>2</sub> heterostructure: a combined experimental and DFT study. *Nanoscale* 9(30):10846–53. <https://doi.org/10.1039/c7nr01451a>
56. Li PP (2022) Study on the design and mechanism of macroscopic superslip in carbon-based two-dimensional materials [D]. University of Chinese Academy of Sciences; University of Chinese Academy of Sciences.
57. Khare HS, Burris DL (2014) Surface and subsurface contributions of oxidation and moisture to room temperature friction of molybdenum disulfide. *Tribol Lett* 53(1):329–336. <https://doi.org/10.1007/s11249-013-0273-0>
58. Uemuer M, Saito K, Nakao KA (1990) Mechanism of vapor effect on friction coefficient of molybdenum disulfide. *Tribol Trans* 33(4):551–556
59. Wang JA, Yu DY, OuYang ML (1994) Degradation of lubrication performance and failure mechanism of molybdenum disulfide sputtered film after storage in humid air. *Tribology* 01:25–32
60. Peterson MB, Johnson RL (1954) Friction and wear investigation of molybdenum disulfide II: Effects of contaminants and method of application, F [C].
61. Lince JR, Frantz PP (2001) Anisotropic oxidation of MoS<sub>2</sub> crystallites studied by angle-resolved X-ray photoelectron spectroscopy. *Tribol Lett* 9(3):211–218. <https://doi.org/10.1023/A:1018869107511>
62. Hilton MR, Fleischauer PD (1990) TEM lattice imaging of the nanostructure of early-growth sputter-deposited MoS<sub>2</sub> solid lubricant films. *J Mater Res* 5(2):406–421. <https://doi.org/10.1557/JMR.1990.0406>
63. Fleischauer PD, Lince JR, Bertrand PA et al (1989) Electronic structure and lubrication properties of molybdenum disulfide: a qualitative molecular orbital approach. *Langmuir* 5(4):1009–1015. <https://doi.org/10.1021/la00088a022>
64. Dimigen H, Hübsch H, Willich P et al (1985) Stoichiometry and friction properties of sputtered MoS<sub>2</sub> layers. *Thin Solid Films* 129(1):79–91. [https://doi.org/10.1016/0040-6090\(85\)90097-5](https://doi.org/10.1016/0040-6090(85)90097-5)
65. Khare HS, Burris DL (2013) The effects of environmental water and oxygen on the temperature-dependent friction of sputtered molybdenum disulfide. *Tribol Lett* 52(3):485–493. <https://doi.org/10.1007/s11249-013-0233-8>
66. Muratore C, Bultman JE, Aouadi SM et al (2011) In situ raman spectroscopy for examination of high temperature tribological processes. *Wear* 270(3):140–145. <https://doi.org/10.1016/j.wear.2010.07.012>
67. Windom BC, Sawyer WG, Hahn DW (2011) A raman spectroscopic study of MoS<sub>2</sub> and MoO<sub>3</sub>: applications to tribological systems. *Tribol Lett* 42(3):301–310. <https://doi.org/10.1007/s11249-011-9774-x>
68. Curry JF, Wilson MA, Luftman HS, et al (2017) Impact of microstructure on MoS<sub>2</sub> oxidation and friction. *ACS Appl Mater Interfaces* 9:28019–28026. <https://doi.org/10.1021/acsami.7b06917>
69. Wang P, Qiao L, Xu J et al (2015) Erosion mechanism of MoS<sub>2</sub>-based films exposed to atomic oxygen environments. *ACS Appl Mater Interfaces* 7(23):12943–12950. <https://doi.org/10.1021/acsami.5b02709>
70. Gao X, Hu M, Sun J et al (2015) Changes in the composition, structure and friction property of sputtered MoS<sub>2</sub> films by LEO environment

- exposure. *Appl Surf Sci* 330:30–38. <https://doi.org/10.1016/j.apsusc.2014.12.175>
71. Tagawa M, Yokota K, Ochi K et al (2012) Comparison of macro and microtribological property of molybdenum disulfide film exposed to LEO space environment. *Tribol Lett* 45(2):349–356. <https://doi.org/10.1007/s11249-011-9893-4>
  72. Lince JR, Loewenthal SH, Clark CS (2019) Tribological and chemical effects of long term humid air exposure on sputter-deposited nano-composite MoS<sub>2</sub> coatings. *Wear* 432–433:202935. <https://doi.org/10.1016/j.wear.2019.202935>
  73. Lince JR (2020) Effective application of solid lubricants in spacecraft mechanisms. *Lubricants* 8(7):74. <https://doi.org/10.3390/lubricants8070074>
  74. Buttery M, Lewis S, Kent A et al (2020) Long-term storage considerations for spacecraft lubricants. *Lubricants* 8(3):32. <https://doi.org/10.3390/lubricants8030032>
  75. Yu DY, Wang JA, OuYang JL (1997) Variations of properties of the MoS<sub>2</sub>-LaF<sub>3</sub> cosputtered and MoS<sub>2</sub>-sputtered films after storage in moist air. *Thin Solid Films* 293(1):1–5. [https://doi.org/10.1016/S0040-6090\(96\)08959-6](https://doi.org/10.1016/S0040-6090(96)08959-6)
  76. Yang Z, Bhowmick S, Sen FG et al (2021) Microscopic and atomistic mechanisms of sliding friction of MoS<sub>2</sub>: effects of undissociated and dissociated H<sub>2</sub>O. *Appl Surf Sci* 563:150270. <https://doi.org/10.1016/j.apsusc.2021.150270>
  77. Serpini E, Rota A, Ballestrazzi A et al (2017) The role of humidity and oxygen on MoS<sub>2</sub> thin films deposited by RF PVD magnetron sputtering. *Surf Coat Technol* 319:345–352. <https://doi.org/10.1016/j.surfcoat.2017.04.006>
  78. Levita G, Righi MC (2017) Effects of water intercalation and tribochemistry on MoS<sub>2</sub> lubricity: an ab initio molecular dynamics investigation. *ChemPhysChem* 18(11):1475–1480. <https://doi.org/10.1002/cphc.201601143>
  79. Ghuman KK, Yadav S, Singh CV (2015) Adsorption and dissociation of H<sub>2</sub>O on monolayered MoS<sub>2</sub> edges: energetics and mechanism from ab initio simulations. *J Phys Chem C* 119:6518–6529. <https://doi.org/10.1021/jp510899m>
  80. Curry JF, Argibay N, Babuska T et al (2016) Highly oriented MoS<sub>2</sub> coatings: tribology and environmental stability. *Tribol Lett* 64(1):11. <https://doi.org/10.1007/s11249-016-0745-0>
  81. Zhao X, Perry SS (2010) The role of water in modifying friction within MoS<sub>2</sub> sliding interfaces. *ACS Appl Mater Interfaces* 2(5):1444–1448. <https://doi.org/10.1021/am100090t>
  82. Lee H, Jeong H, Suh J et al (2019) Nanoscale friction on confined water layers intercalated between MoS<sub>2</sub> flakes and silica. *The J Phys Chem C*. <https://doi.org/10.1021/acs.jpcc.8b11426>
  83. Kubart T, Polcar T, Kopecký L et al (2005) Temperature dependence of tribological properties of MoS<sub>2</sub> and MoSe<sub>2</sub> coatings. *Surf Coat Technol* 193(1):230–233. <https://doi.org/10.1016/j.surfcoat.2004.08.146>
  84. Arslan E, Totik Y, Bayrak O et al (2009) High temperature friction and wear behavior of MoS<sub>2</sub>/Nb coating in ambient air. *J Coat Technol Res* 7(1):131. <https://doi.org/10.1007/s11998-009-9171-7>
  85. Brainard WA (1969) The thermal stability and friction of the disulfides, diselenides, and ditellurides of molybdenum and tungsten in vacuum, F [C].
  86. Wang R, Li HG, Ji L, Liu XH, Sun CF (2022) Tribological properties of MoS<sub>2</sub>-based composite films at vacuum and high temperature and their mechanism. *Tribology* 43(1):73–82. <https://doi.org/10.16078/j.tribology.2021296>
  87. Wang JH, Yang J (2005) Characterization of magnetron sputtered MoS<sub>2</sub> thin films. *Lubric Seal* 30(06):12–4+23
  88. Banerji A, Bhowmick S, Alpas AT (2017) Role of temperature on tribological behaviour of Ti containing MoS<sub>2</sub> coating against aluminum alloys. *Surf Coat Technol* 314:2–12. <https://doi.org/10.1016/j.surfcoat.2016.09.044>
  89. Sun G, Bhowmick S, Alpas AT (2017) Effect of atmosphere and temperature on the tribological behavior of the Ti containing MoS<sub>2</sub> coatings against aluminum. *Tribol Lett* 65(4):158. <https://doi.org/10.1007/s11249-017-0934-5>
  90. Paul A, Singh H, Mutyala K C, et al (2018) An Improved Solid Lubricant for Bearings Operating in Space and Terrestrial Environments, F, [C].
  91. Karapetyan SS, Silin AA (1976) Temperature dependence of friction coefficient of molybdenum disulfide in vacuum in the 300–80 °K range. *Soviet Phys Doklady* 229:1
  92. Lince J, Kim H, Kirsch J, et al (2016) Low-temperature friction variation of MoS<sub>2</sub>-based lubricants [M].
  93. Zhao X, Phillpot SR, Sawyer WG et al (2009) Transition from thermal to athermal friction under cryogenic conditions. *Phys Rev Lett* 102(18):186102. <https://doi.org/10.1103/PhysRevLett.102.186102>
  94. Curry JF, Hinkle AR, Babuska TF et al (2018) Atomistic origins of temperature-dependent shear strength in 2D materials. *ACS Appl Nano Mater* 1(10):5401–5407. <https://doi.org/10.1021/acsanm.8b01454>
  95. Duncle CG, Aggleton M, Glassman J et al (2011) Friction of molybdenum disulfide–titanium films under cryogenic vacuum conditions. *Tribol Int* 44(12):1819–1826. <https://doi.org/10.1016/j.triboint.2011.07.010>
  96. Babuska TF, Pitenis AA, Jones MR et al (2016) Temperature-dependent friction and wear behavior of PTFE and MoS<sub>2</sub>. *Tribol Lett* 63(2):15. <https://doi.org/10.1007/s11249-016-0702-y>
  97. Colbert RS, Sawyer WG (2010) Thermal dependence of the wear of molybdenum disulfide coatings. *Wear* 269(11):719–723. <https://doi.org/10.1016/j.wear.2010.07.008>
  98. Ju H, Wang R, Ding N et al (2020) Improvement on the oxidation resistance and tribological properties of molybdenum disulfide film by doping nitrogen. *Mater Des* 186:108300. <https://doi.org/10.1016/j.matdes.2019.108300>
  99. Kim E, Ko C, Kim K et al (2016) Site selective doping of ultrathin metal dichalcogenides by laser-assisted reaction. *Adv Mater* 28(2):341–346. <https://doi.org/10.1002/adma.201503945>
  100. Sun WD, Gu XL, Yang LN et al (2020) Effect of boron content on the structure, mechanical and tribological properties of sputtered Mo–S–B films. *Surf Coat Technol* 399:126140. <https://doi.org/10.1016/j.surfcoat.2020.126140>
  101. Teer DG (2001) New solid lubricant coatings. *Wear* 251(1):1068–1074. [https://doi.org/10.1016/S0043-1648\(01\)00764-5](https://doi.org/10.1016/S0043-1648(01)00764-5)
  102. Lu X, Yan M, Yan Z et al (2021) Exploring the atmospheric tribological properties of MoS<sub>2</sub>-(Cr, Nb, Ti, Al, V) composite coatings by high throughput preparation method. *Tribol Int* 156:106844. <https://doi.org/10.1016/j.triboint.2020.106844>
  103. Stoyanov P, Chromik RR, Goldbaum D et al (2010) Microtribological performance of Au–MoS<sub>2</sub> and Ti–MoS<sub>2</sub> coatings with varying contact pressure. *Tribol Lett* 40(1):199–211. <https://doi.org/10.1007/s11249-010-9657-6>
  104. Wahl KJ, Dunn DN, Singer IL (1999) Wear behavior of Pb–Mo–S solid lubricating coatings. *Wear* 230(2):175–183. [https://doi.org/10.1016/S0043-1648\(99\)00100-3](https://doi.org/10.1016/S0043-1648(99)00100-3)
  105. Zabinski JS, Donley MS, Dyhouse VJ et al (1992) Chemical and tribological characterization of PbO&MoS<sub>2</sub> films grown by pulsed laser deposition. *Thin Solid Films* 214(2):156–163. [https://doi.org/10.1016/0040-6090\(92\)90764-3](https://doi.org/10.1016/0040-6090(92)90764-3)
  106. Yu DY, Wang JA, Yang JLO (1997) Variations of properties of the MoS<sub>2</sub>-LaF<sub>3</sub> cosputtered and MoS<sub>2</sub>-sputtered films after storage in moist air. *Thin Solid Films* 293(1):1–5. [https://doi.org/10.1016/S0040-6090\(96\)08959-6](https://doi.org/10.1016/S0040-6090(96)08959-6)
  107. Zhang C, Yang B, Wang J et al (2019) Microstructure and friction behavior of LaF<sub>3</sub> doped Ti–MoS<sub>2</sub> composite thin films deposited by unbalanced magnetron sputtering. *Surf Coat Technol* 359:334–341. <https://doi.org/10.1016/j.surfcoat.2018.12.041>
  108. W M J (1969) A theory and tester measurement correlation about MoS<sub>2</sub> dry film lubricant wear, F, [C].
  109. Bidev F, Baran Ö, Arslan E et al (2013) Adhesion and fatigue properties of Ti/TiB<sub>2</sub>/MoS<sub>2</sub> graded-composite coatings deposited by closed-field unbalanced magnetron sputtering. *Surf Coatings Technol* 215:266–271. <https://doi.org/10.1016/j.surfcoat.2012.08.091>
  110. Singh H, Mutyala KC, Evans RD et al (2017) An atom probe tomography investigation of Ti–MoS<sub>2</sub> and MoS<sub>2</sub>-Sb<sub>2</sub>O<sub>3</sub>-Au films. *J Mater Res* 32(9):1710–1717. <https://doi.org/10.1557/jmr.2017.35>
  111. Wang P, Qiao L, Xu J, Li WX et al (2015) Erosion mechanism of MoS<sub>2</sub>-based films exposed to atomic oxygen environments. *Appl Mater Interfaces* 7:12943–12950. <https://doi.org/10.1021/acsami.5b02709>
  112. Hsu W-K, Zhu YQ, Yao N et al (2001) Titanium-doped molybdenum disulfide nanostructures. *Adv Func Mater* 11:69–74. [https://doi.org/10.1002/1616-3028\(200102\)11:13.0.CO;2-D](https://doi.org/10.1002/1616-3028(200102)11:13.0.CO;2-D)

113. Scharf TW, Goeke RS, Kotula PG et al (2013) Synthesis of au-MoS<sub>2</sub> nanocomposites: thermal and friction-induced changes to the structure. *ACS Appl Mater Interfaces* 5(22):11762–11767. <https://doi.org/10.1021/am4034476>
114. Ye Y, Chen J, Zhou H (2009) Microstructure, tribological behavior, and corrosion-resistant performance of bonded MoS<sub>2</sub> solid lubricating film filled with Nano-LaF<sub>3</sub>. *J Dispersion Sci Technol* 30(4):488–494. <https://doi.org/10.1080/01932690802549039>
115. Lince JR, Kim HI, Adams PM et al (2009) Nanostructural, electrical, and tribological properties of composite Au–MoS<sub>2</sub> coatings. *Thin Solid Films* 517(18):5516–5522. <https://doi.org/10.1016/j.tsf.2009.03.210>
116. Lince JR (2004) Tribology of co-sputtered nanocomposite Au/MoS<sub>2</sub> solid lubricant films over a wide contact stress range. *Tribol Lett* 17(3):419–428. <https://doi.org/10.1023/B:TRIL.0000044490.03462.6e>
117. Li B, Wan H, Ye Y et al (2017) Investigating the effect of LaF<sub>3</sub> on the tribological performances of an environment friendly hydrophilic polyamide imide resin bonded solid lubricating coating. *Tribol Int* 116:164–171. <https://doi.org/10.1016/j.triboint.2017.07.014>
118. Ye YP, Chen JM, Zhou HD (2009) Influence of nanometer lanthanum fluoride on friction and wear behaviors of bonded molybdenum disulfide solid lubricating films. *Surf Coat Technol* 203(9):1121–1126. <https://doi.org/10.1016/j.surfcoat.2008.10.00>
119. Zhang X, Luster B, Church A et al (2009) Carbon Nanotube–MoS<sub>2</sub> composites as solid lubricants. *ACS Appl Mater Interfaces* 1(3):735–739. <https://doi.org/10.1021/am800240e>
120. Zhao X, Lu Z, Zhang G et al (2018) Self-adaptive MoS<sub>2</sub>-Pb-Ti film for vacuum and humid air. *Surf Coat Technol* 345:152–166. <https://doi.org/10.1016/j.surfcoat.2018.04.022>
121. Aouadi SM, Paudel Y, Simonson WJ et al (2009) Tribological investigation of adaptive Mo<sub>2</sub>N/MoS<sub>2</sub>/Ag coatings with high sulfur content. *Surf Coat Technol* 203(10):1304–1309. <https://doi.org/10.1016/j.surfcoat.2008.10.040>

### Publisher's Note

Springer Nature remains neutral with regard to jurisdictional claims in published maps and institutional affiliations.